In presenting the dissertation as a partial fulfillment of the requirements for an advanced degree from the Georgia Institute of Technology, I agree that the Library of the Institute shall make it available for inspection and circulation in accordance with its regulations governing materials of this type. I agree that permission to copy from, or to publish from, this dissertation may be granted by the professor under whose direction it was written, or, in his absence, by the Dean of the Graduate Division when such copying or publication is solely for scholarly purposes and does not involve potential financial gain. It is understood that any copying from, or publication of, this dissertation which involves potential financial gain will not be allowed without written permission.

[redacted]

7/25/68

A FLUIDIC TEMPERATURE CONTROL SYSTEM UTILIZING A HILSCH TUBE

A THESIS

Presented to

The Faculty of the Graduate Division

by

Richard Murray Baldwin

In Partial Fulfillment

of the Requirements for the Degree

Master of Science in Mechanical Engineering

Georgia Institute of Technology

May, 1969

A FLUDIC TEMPERATURE CONTROL SYSTEM

UTILIZING A HILSCH TUBE

Approved:

Chairman

Date approved by Chairman:

ACKNOWLEDGMENTS

The author wishes to express sincere appreciation to those who made this study possible. Special thanks are extended to Dr. Steve Dickerson, the author's thesis and faculty advisor, for his interest and guidance in this research, and to Dr. W. Z. Black for his counseling and assistance during Dr. Dickerson's summer absence.

Gratitude is also extended to Mrs. Louise Barge for her excellent typing of this final draft and to Richard A. Whisnant for handling the publication of this thesis in the author's absence.

Finally, the author wishes to thank the Department of Mechanical Engineering for the Graduate Assistantship Grant which made it possible for him to attend graduate school.

TABLE OF CONTENTS

Page

APPENDICES

LIST OF ILLUSTRATIONS

LIST OF SYMBOLS

A orifice area.

b width of bimetal.

C heat transfer constant.

C_d orifice coefficient for fixed orifices.

C_f orifice coefficient for flapper orifices.

c_p heat capacity of air at constant pressure.

D_f free thermal deflection of bimetal.

D_l deflection of bimetal caused by opposing load.

d diameter of an orifice.

F air flow-force on the flapper.

F_T load on the bimetal lever.

g acceleration of gravity.

K ratio of specific heats.

K mass ratio = $(\dot{m}_{cl} + \dot{m}_{cr})/\dot{m}_o$.

K' $\frac{K}{R}\sqrt{g}\left(\frac{2}{K+1}\right)^{(K+1)/(K-1)}$

K_{DC} bimetal coil deflection constant.

K_{PC} bimetal coil torque constant.

k in an amplifier, the ratio of the width of the control orifice to the width of the power orifice.

L (1) in the bimetal, the length of the bimetal strip.

(2) in the sensor, the distance between flapper nozzles

(less thickness of flapper).

(3) in an amplifier, the distance from the power nozzle receiving aperature.

m specific deflection of the bimetal $(D_f - D_1)/D_f$.

$\dot{M}$ or $\dot{m}$ mass flow of air.

$$N_{12} \quad \frac{(P_2/P_1)^{2/K} - (P_2/P_1)^{(k-1)/K}}{\frac{K-1}{K} \quad \frac{2}{K\ 1}^{(K\ 1)/(K-1)}}^{1/2}$$

P air pressure.

R universal gas constant

r on the bimetal, the radius to the point load application.

T temperature.

t thickness of the bimetal.

w width of an amplifier channel or orifice.

x deflection of the bimetal.

θ angle of deflection of the power jet in an amplifier.

ρ density of fluid.

Subscripts

A designation for the parameters on one side of the temperature sensor.

a, amb ambient conditions.

B designation for parameters on the side opposite A in the temperature sensor.

1 left.

m,mix mixing tube conditions.

o	output conditions, or relating to the power orifice of an amplifier.
out	output conditions.
r	right.
s	supply.
1	designation for parameters relating to the first orifice in either side of the temperature sensor.
2	designation for parameters relating to the flapper orifice on either side of the temperature sensor.
3	designation for parameters relating to the output orifice on either side of the temperature sensor.

SUMMARY

The object of this study is to apply a Hilsch tube as a pure fluid device and to utilize it both as a heat source and heat sink for a fluidic temperature control system. The hot and cold air produced by the vortex tube are passed through two proportional fluidic controllers and mixed in a container where the ambient temperature is to be controlled. A fluidic temperature transducer which has a thermostatic bimetal sensor provides the feedback signal. This signal is amplified by a cascade of fluidic proportional amplifiers to provide the control inputs to the Hilsch tube flow control elements. These elements regulate the amount of hot and cold air that flow into the container, and thus regulate the temperature.

In the original design from which the fluidic amplifiers were constructed, some improper impedance matching calculations were made. The proper amplifier geometry has been calculated and is presented in Appendix III. This impedance mismatch caused the overall gain of the control system to be very low. The response of each component is presented, however.

The thermal efficiency of the system is rather low, but this can be improved. There is also some need to decrease the rather high air power consumption of the sytem.

The control system is very reliable since it has no moving parts and only two necessary energy transducers, the Hilsch tube and the temperature sensor, between heat and fluid flow. Auxiliary transducers

and power supplies are elimintated by utilizing air for both the heat transfer and contrclling media.

CHAPTER I

INTRODUCTION

The Control System

Since the development of pure-fluid devices in the early 1960's, the field now known as fluidics has become quite important in automatic control. The use of a fluid as the working medium in these control devices leads to the idea that fluidics might be easily adapted to the temperature control of a fluid. Using fluidic devices, a temperature control system might be conceived which used the same fluid as the controlled medium and working medium. More specifically, it should be possible to build a system which controlled the temperature and flow of a fluid by means of the fluid itself.

If the fluid selected for the system is a gas, particularly air, then the hot and cold gas necessary for the control system may be produced by a Hilsch tube. The Hilsch tube is also a pure-fluid device, although it was first developed in the 1930's, long before fluidics was conceived. In general, a Hilsch tube is a device which separates a compressed gas jet at room temperature into a hot stream and a cold stream by vortex action.

Thus, by utilizing a Hilsch tube and several fluidic elements, this research proposes to design and construct a fluidic temperature control system to regulate the air temperature in a small enclosure. From a high-pressure air supply, a Hilsch tube will produce hot and cold

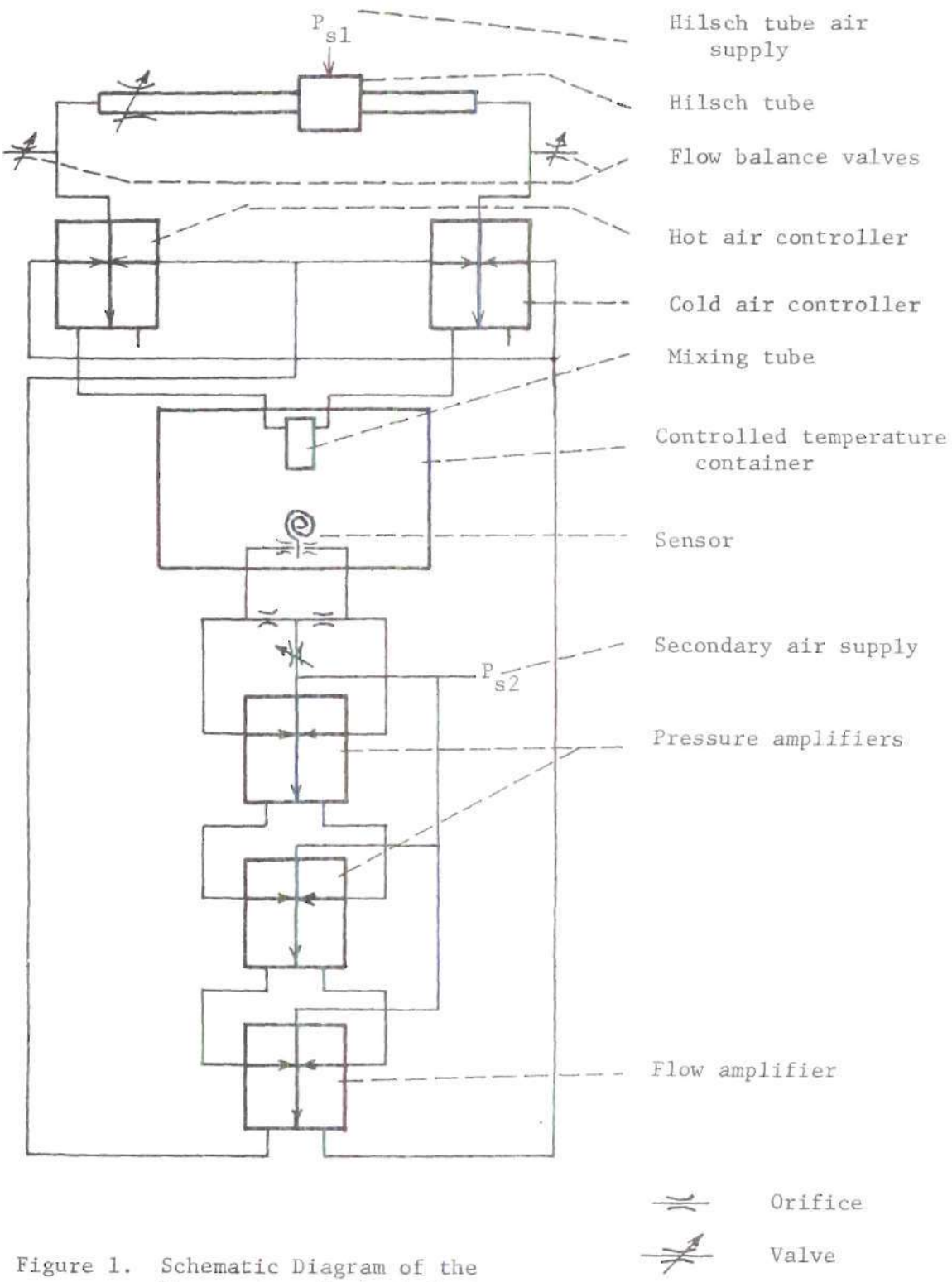

Figure 1. Schematic Diagram of the Temperature Control System

air jets. The flow of these jets into the mixing container where the air temperature is to be regulated will be controlled by two fluidic proportional amplifiers. A temperature sensor and fluidic amplifiers will provide the feedback to the control ports of the proportional controllers (see Fig. 1). A bimetallic strip will serve as the temperature sensor, as explained below.

With the exception of the mechanical deflection of the bimetal strip, the system will be entirely fluidic and have no moving parts. For this reason it should be very reliable and free from the need for much service. The manual adjustments to be made are adjusting the back pressure on the Hilsch tube for the optimum temperature differential, balancing the hot and cold flows to a good operating point in the controllers, zeroing the temperature sensor at the desired temperature, and setting the regulators on the inlet air flow. All of these will be adjusted only once for a given operating condition and require no further variation, as long as the air supply does not vary.

Literature Review

Hilsch Tube

M. Georges Joseph Ranque, a French metallurgist, first reported on vortex tubes in 1931 in a paper read to the Societe Francaise de Physique (1). He first noticed the vortex cooling effect in connection with cyclone separators, and built a device to duplicate the effect. He applied for French and U. S. patents on the device in 1931 and 1932, respectively. Later research proved the vortex to be less efficient than an ordinary refrigerator and nothing more was heard of the device until 1946.

During the Second World War a German low-temperature physicist named Rudolf Hilsch perfected the device and wrote a description of it in 1946. After the war several American scientists visited Hilsch's laboratory at Erlangen University and found the vortex tube and his thesis. Hilsch's thesis (2) was translated by I. Estermann, of the Carnegie Institute of Technology, and its circulation started a flood of research to explain the mechanism of the "Hilsch tube" and to find a practical use for it. There were several varying theories on the operation of the device (16-24), but very few practical applications.

There are two major reasons for the lack of applications for this apparently marvelous instrument: 1) it has a low cooling efficiency as a refrigerator and 2) the applications have attempted to use only the cold air side for cooling or refrigeration, neglecting the warm air. Not until quite recently has there developed any interest in the vortex tube as both a heat source and sink (4). No known attempt has previously been made to apply the Hilsch tube to fluidic uses.

Fluidics

Research in pure-fluid systems first began in 1959 at the Harry Diamond Ordnance Fuze Laboratories using the inventions of B. M. Horton, R. W. Warren, and R. E. Bowles (5). During the development of pure-fluid devices, many control and amplification components were developed to perform different functions. One of the most important devices and the only one used in this system is Horton's Stream Interaction Amplifier or proportional fluid amplifier. In this control system the proportional amplifier is used for two different functions: 1) to amplify the feedback control signal, and 2) to proportionally control the flow of the hot and

cold jets from the Hilsch tube.

Fluidic amplifier design is still the object of intense research. Most of the critical parameters and their effects are known, but there still are no well-defined models which meet all design criteria (6-8).

Temperature Sensor

Some literature research was necessary in order to determine what type of temperature sensor could best be adapted to a pure fluid system with satisfactory sensitivity. Generally, a sensor with the following qualifications was sought:

It must be able to sense at least a 2°F temperature change between the range of -50°F and 200°F.

It must be an active device that can produce an output proportional to the temperature change.

The output should preferably be an air pressure or flow, eliminating the need for a transducer.

It should have a high reliability. This infers few, if any, moving parts.

It should be as simple and compact as possible.

These restrictions immediately eliminated thermocouples and all electrical sensing devices because they would require a transducer. They also eliminated thermomenters and other sensors which had no usable output. The first sensor actually considered turned out to be the best from every standpoint - a thermostatic bimetal. It could be designed to meet all of the qualifications above.

As explained more fully later, a bimetal was designed which moved a flapper in front of an orifice as it deflected with temperature changes.

This idea was derived from the flapper valve pneumatic controllers discussed by Blackburn, Rethoff, and Shearer, (10), and By Gibson and Tuteur (12). The motion of the flapper varied the pressure between two orifies in series. This pressure was tapped and utilized as the output signal. A second set of orifices was placed on the opposite side of the flapper, so that as the pressure in one side went up, the pressure in the other side went down. The pressures change between the two sides was amplified through three cascaded proportional amplifiers and used as the feedback control signal.

Another interesting temperature sensor was found which was completely fluidic (9). It employed a fluidic oscillator whose frequency varied with the temperature change of the gas it operated on. When beat against an oscillator of known frequency, it could be calibrated to the temperature. This sensor was not selected for the present system because it required considerable auxiliary pulse modulation equipment to obtain an output and was bulky and complex. This sensor alone was more complex than the entire system here being designed.

CHAPTER II

THEORY OF OPERATION

Taking each system component individually, let us now analyze theoretically how and why the system operates.

Hilsch Tube

Despite the volumes of theoretical and experimental literature published in the last 35 years on the vortex tube, there is still much dissension over the mechanism involved. There is a certain amount of agreement, however, on the tube's principle. Air at room temperature and high pressure is passed through a nozzle entering the circular tube tangentially and forming a vortex. Internal friction between the molecules rotating in the vortex attempts to reduce all of the molecules to the same angular velocity. This causes the molecules at the core to slow down and those at the periphery to speed up which amounts to the flow of work or kinetic energy from the center to the outer edge of the vortex. The resulting temperature gradient tends to cause heat flow in the opposite direction, but not nearly as rapidly.

An additional cooling effect comes from the centrifugal force of the vortex itself. It causes a pressure gradient of hot, dense gas at the periphery and cold, lower pressure gas at the core. Any molecule dropping to the center of the spiral is thus cooled by expansion from a high pressure layer to a lower pressure layer.

The result is that while the gas is spiraling down the tube, a core of cold air is produced at the central axis and an annulus of

hot air is formed at the periphery. Under these conditions, the low pressure air at the core would draw atmospheric air into the tube through the central orifice. To avoid this a regulating valve is placed downstream in the hot arm of the tube to produce a back pressure in the chamber forcing the cold air to escape out the orifice. Thus, hot air is obtained at one end of the tube and cold air at the other. The back pressure valve on the tube may be "tuned" for an extreme temperature with low flow at either end, or for a higher flow rate but less extreme temperatures.

Proportional Amplifier

The proportional amplifier is also variously known as a stream-interaction or stream-deflection amplifier, analog amplifier, and beam deflection fluid amplifier. All of these names indicate to some extent its purpose or method of operation. At the exit of the supply tube, two smaller control jets are arranged at right angles to the power jet (see Fig. 2). The interaction of these two jets on the power jet causes it to deflect in the direction of the smaller control jet. This occurs through momentum interchange of the small jets on the large one. The two downstream output collectors receive fractions of the total flow in proportion to the amount of deflection of the power jet.

The dimensions of the proportional amplifier may be varied slightly in order to emphasize either pressure gain, flow gain, or proportional division of the power jet. In this system proportional division of the power jet is employed in controlling the Hilsch tube flow and Corning proportional elements are used to obtain pressure amplification in the feedback loop. Flow gain is obtained in an intermediate amplifier

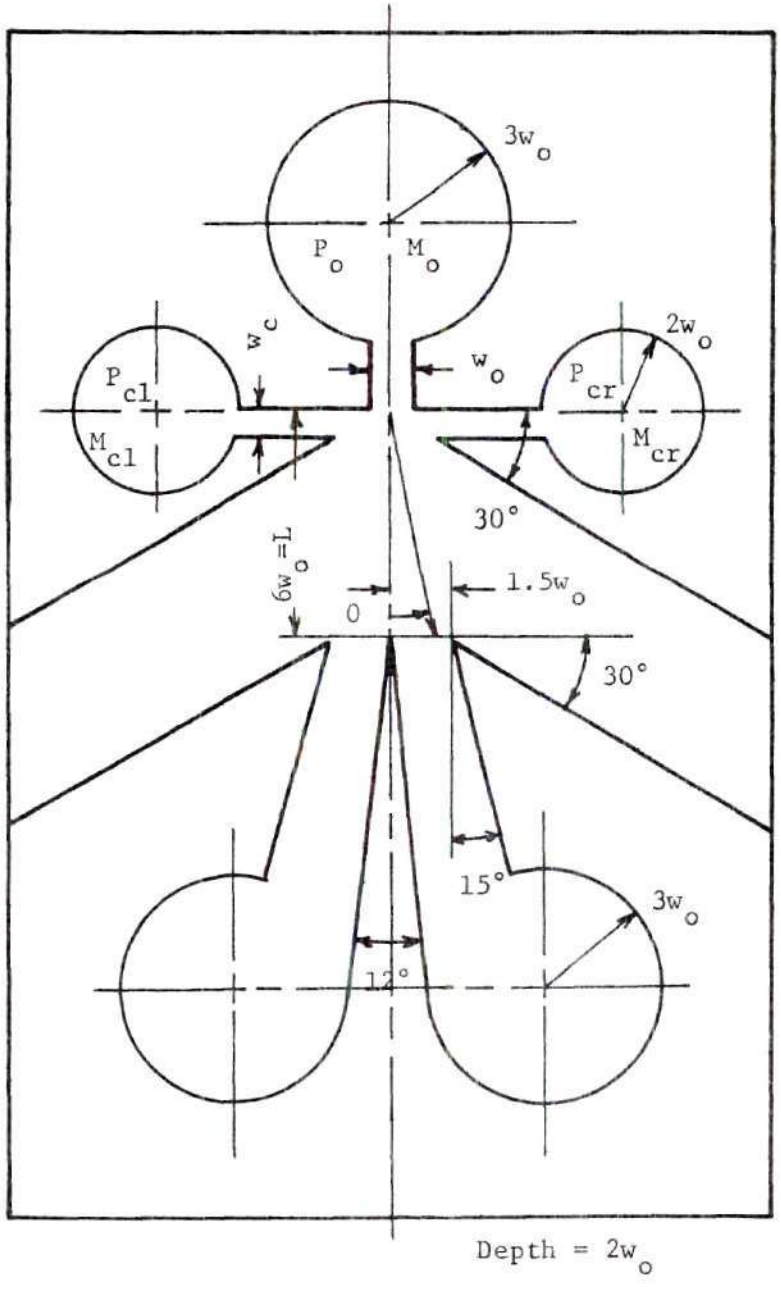

Figure 2. Enlarged Diagram of a Fluidic Proportional Amplifier Showing Typical Size Ratios

and the controllers.

Temperature Sensor

The temperature sensor used as the feedback element in the system is essentially a modification of the flapper valve principle often employed in pneumatic and hydraulic systems (10-12). Its electrical analogy is a voltage divider circuit with a variable load resistor.

As the flow through the flapper valve varies with the motion of the flapper, the pressure in the upstream chamber between the orifices varies inversely (see Fig. 13). This pressure change causes a proportional change of flow in the branch connection, which is utilized as the control jet. The flapper is mounted on a spiralled bimetallic strip which deflects with ambient temperature changes, causing the motion of the flapper.

Another set of orifices are placed on the other side of the flapper. This set produces a control jet which varies inversely to the first one. The differential of the control pressures may be used to control a proportional amplifier which amplifies the small control pressure up to a pressure level that can be used to control the Hilsch tube flows. Two Corning proportional pressure amplifiers and a flow amplifier in cascade are used for this purpose.

CHAPTER III

DESIGN MODEL

The action of most physical systems can be expressed by mathematical equations or models. From these models the proper size for certain dimensions and physical parameters in relation to the rest of the system can be determined. This chapter deals with the derivation and solution of equations and models which represent the control system.

Hilsch Tube

As previously discussed, the mathematical analysis of the Hilsch tube is quite uncertain and very complex at best. Instead of designing a Hilsch tube, a previously published design by Blaber (13) having known characteristics was duplicated (Fig. 3). At four atmospheres inlet pressure, the maximum temperature differences between the hot and cold outlet sides should be about 140°F, according to Balber's data. Maintaining this temperature difference while varying the back pressure, the cold outlet temperature should vary from 5°F to 40°F as the hot outlet varies from 140°F to 190°F.

The Hilsch tube was constructed from teflon rod and tubing. This material was selected because of its temperature insulation qualities and its ease of machining. The parts were fastened with epoxy glue, then reinforced with mechanical fasteners.

It was discovered during the process of experimenting with the Hilsch tube that the hot outlet tube, which was supposed to be about

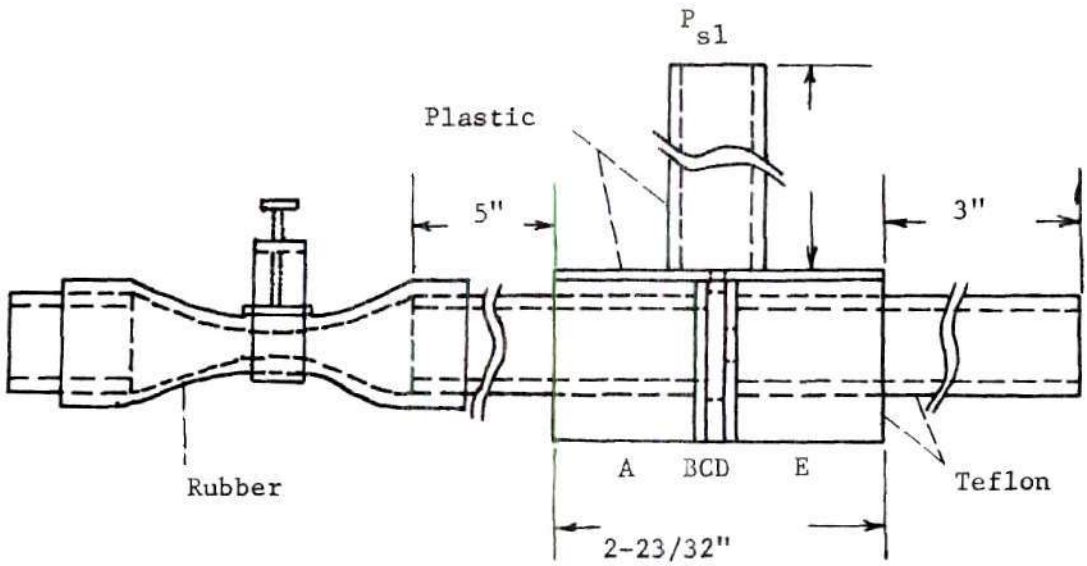

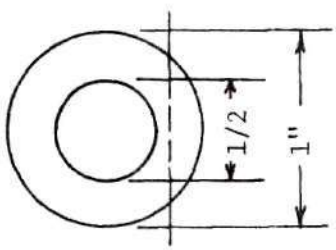

Parts A & E

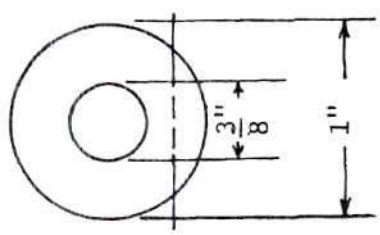

Part B

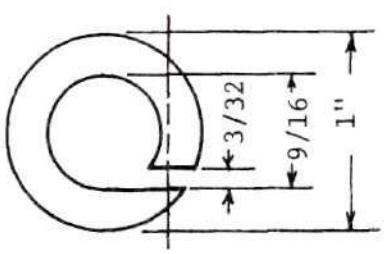

Part C

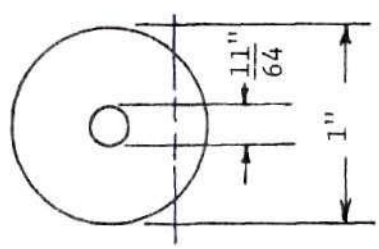

Part D

Figure 3. Hilsch Tube Construction Drawing

15-20 inches long, could be shortened to about 6 inches without noticeably affecting the temperatures of the outputs. This made the device easier to mount for display.

A screw clamp on a piece of rubber tubing in the hot outlet line provided the feedback pressure regulation. Also, the output flows into the proportional controllers could be adjusted to a good operating point by partially opening a similar screw clamp arrangement tapped into each temperature line between the Hilsch tube and the controllers.

Temperature Sensor

The design of the temperature sensor begins with the bimetallic coil. This is the only purely linear element in the system. The equations used to design this component were obtained from the W.M. Chace Co. Thermostatic Bimetal Design Catalog (14) (see Appendix I). The Chace Company also provided free samples of their No. 2400 bimetallic strip which were used to fabricate the sensor.

The fluidic portion of the sensor can be expressed mathematically by the equations shown in Appendix II.. These equations are extemely non-linear and cannot be easily linearized or expressed in transfer function form. To make the solutions of these equations useful, they were solved graphically, as shown in the appendix.

In order to minimize the power consumption of the sensor and the temperature effects of its exhaust air, the orifices were made as small as practical. All four orifices were drilled in 3/16 inch brass rod with a number 60 drill bit (0.040 in.). The temperature effects of the exhaust air on the bimetal were reduced by attaching a plastic lever arm to the bimetal to serve as the flapper. Also, a plastic shield was placed between the bimetal and the flapper valves to direct the exhaust air away

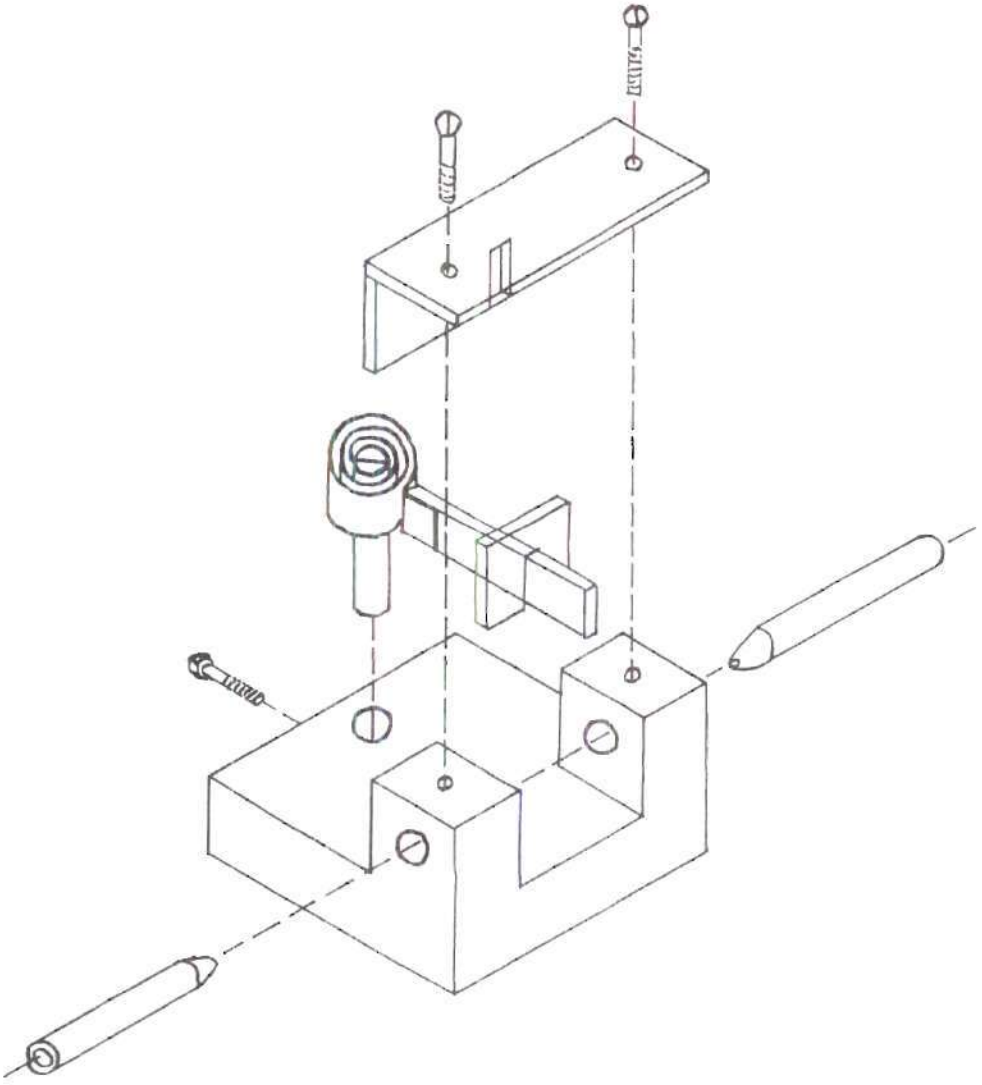

Figure 4. Temperature Sensor Schematic (approximately actual size).

from the bimetal. The air supply pressure was kept low (4-5 psig) to minimize the amount of air consumed by the sensor.

Theoretically the sensor is composed of three orifices in each side of the circuit. In practice, however, the control orifice of the first stage pressure amplifier serves as the orifice for the branch of the circuit that provides the control pressure.

The flapper orifice spacing determines, in part, the sensitivity of the sensor. For good response, the flapper should not be more than one orifice diameter from the nozzle. If the distance between the nozzles, excluding the thickness of the flapper, is greater than one orifice diameter, only the nozzle toward which the flapper is deflected will respond well. If the nozzle separation is greater than two orifice diameters, a dead zone will be produced in the center where neither nozzle will respond. If the nozzle separation is made about one orifice diameter or less, both nozzles will respond to a flapper deflection in the opposite manner. Good response was found for the sensor with a nozzle separation of about 1/32 inch. The separation distance may be varied by loosening two set screws and moving the nozzles.

The sensor may be set to a desired temperature by biasing the flapper off center between the nozzles. Unless time is taken to calibrate the bimetal, which might be tedious, the amount of offset must be determined by trial and error. An alternate method would be to expose the sensor to the desired temperature and then zero the flapper to balance the control pressures. The bimetal may be adjusted by loosening a set screw and rotating the bimetal holder.

Fluid Amplifiers

The design calculations for the fluid amplifiers came largely from models presented by Dexter (6) and Reilly (7) and from fundamental fluid flow equations. The design model equations are presented in Appendix III.

The Corning amplifiers used in the first two stages of the feedback can each provide maximum pressure gains of five and six and at typical operating levels the gains are between two and four. These figures are from the manufacturer's data sheet as shown on pages 30 and 31.

After the feedback pressure is built up to a substantial level (about 3 psig) by the Corning units, it can be used to provide the control signal to a flow amplifier. The flow amplifier uses a high pressure, low flow signal to control a high flow supply jet. The result is a much higher flow output at a lower pressure level. The power jet on this flow amplifier was designed for a 10 psig pressure drop across the power orifice. This provides a high flow using the same 10 psig supply pressure provided to the Corning amplifiers. The size of the control nozzles is determined by impedance matching and pressure ratios, as shown in Appendix III.

The Hilsch tube controlling amplifiers were designed using about the same models and design criteria as the flow amplifier, except that different parameters were known initially (also in Appendix III).

A few dimensional alterations were necessary between the design values and the sizes that could actually be fabricated. The two controlling amplifiers were designed to have control ports 0.040 inches wide. These amplifiers were were to be machined on a vertical milling machine and the smallest end mill that was available was 1/16 inch. This means that it was necessary to make the control port areas 50 percent larger

than was designed. Also, it was planned to machine the amplifiers out of plastic to reduce thermal losses. Plastic is not easy to mill, however, so aluminum was accepted as a substitute material.

In order to construct the smaller flow amplifier, it was necessary to find an easy way to fabricate an amplifier with small passages, preferrably from plastic. This was accomplished by cutting the amplifier profile out of a sheet of plastic, sawing it into sections, and gluing the sections in the proper proximity on a second piece of plastic. A feeler gauge was used to measure passage widths, but some difficulty was still encountered in duplicating the design calculations. As in the other amplifiers, a plastic cover plate was bolted over the open face of the amplifier. The plastic tubing connectors were made perpendicularly through the back of the amplifier by means of metal tubing.

Temperature Controlled Environment

The container in which the temperature was controlled had few requirements concerning its design. The main limitation was the amount of cooling or heating which had to be provided for it by the control system. The heat balance equations for the temperature controlled box are shown in Appendix IV.

The container used in this experiment had a volume of about 130 cubic inches and was made of cardboard with a vent in the top. Holes were cut in the box for the two sensor air tubes, and ambient temperature measuring thermomenter, and the air mixing tube.

The mixing tube was a device designed so that the net temperature of the hot and cold air entering the box could be measured. It consisted

of a paper tube about three-quarters of an inch in diameter and three inches long, with one end blocked. At the blocked end, the hot and cold air hoses entered the opposite sides of the tube. The two air streams mixed as they travelled down the tube and their resultant temperature was measured by a thermocouple near the open end of the tube.

Inside the box were placed the sensor, a heater, a radiation heat shield, and the ambient temperature thermometer bulb. The radiation heat shield was simply a piece of cardboard which protected the temperature sensing devices from direct heat radiating from the tensor lamp which served as the heater. Convective heating (or cooling) was allowed to pass freely around the shield.

A second thermometer was placed with its bulb in the exhaust vent on top of the box. It measured the outlet air temperature.

CHAPTER IV

TESTS AND RESULTS

Control System

The actual response of each component in the block diagram could not be determined independently because certain parameters, such as flow rates, could not be accurately measured. To solve this problem, some of the components were lumped together and their combined open-loop response was determined.

The flow amplifier and controllers were among the components which were lumped with other parts to determine the system response. Open-loop Test A was made to determine the mixing temperature that resulted for a given pressure differential placed across the flow amplifier control ports (see Figs. 21-25). At the same time the mixing temperature, the ambient temperature, and the exit temperature in the box were plotted against time to determine the time response of the box.

Open-loop Test B (Figs. 26-29) was the same as Test A except that the control pressure was placed into the opposite (left) side of the flow amplifier. In addition, the output pressures on either side of the sensor were recorded. Thus the sensor response would also be observed.

Test C determines the open-loop response from the box through the sensor and pressure amplifiers. The heater was placed in the box and turned on; the flow amplifier was turned off. When the box heated up to a steady-state condition the lamp was turned off and the mixing, ambient,

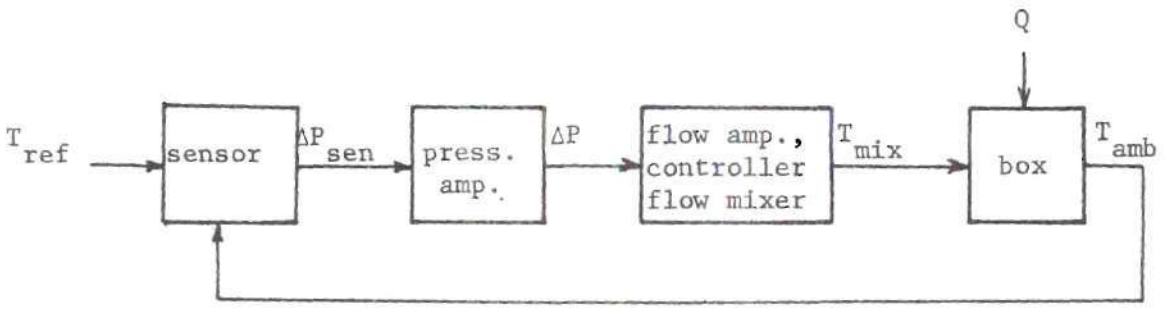

Closed-loop block diagram

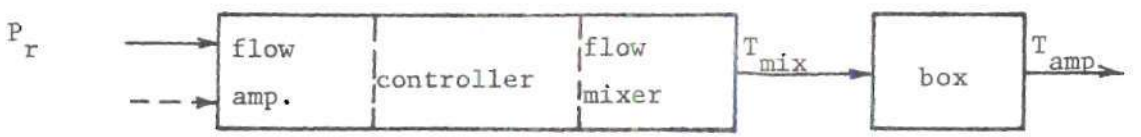

Open-loop Test A

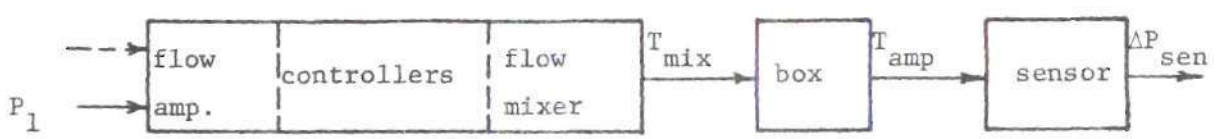

Open-loop Test B

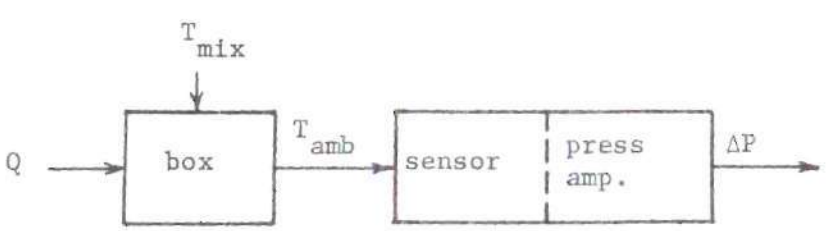

Open-loop Test C

Figure 5. Block Diagrams of Closed-loop and Open-loop Experimental Model Tests

and outlet temperatures, as well as the Corning amplifier output pressures were recorded as a function of time. When the cool steady-state condition was reached, the reverse system response was recorded by turning the heater on again.

The final test was the closed-loop response. In this test the entire loop was closed and every component activated. The data recorded were the mixing, ambient, and outlet box temperatures, the sensor output pressures, the pressure amplifier outputs, and the response time.

The results of these tests are compared with the mathematical models and the differences discussed in the following chapter.

Hilsch Tube

The Hilsch tube seems to have a reasonably linear relationship between the inlet pressure and the difference in the outlet temperatures. Over a pressure range from about 36 to 60 psig the output temperature difference is about 100°F with a variation of plus or minus 10 percent, depending on the back pressure setting and the inlet pressure. The best operating point seems to be 40 psig supply pressure and the back pressure adjusted for a maximum hot temperature output. Actual numerical values of the output temperatures in this operating range are 130-155°F on the hot side and 25-45°F on the cold side.

CHAPTER V

COMPARISON OF THE MATHEMATICAL AND EXPERIMENTAL MODELS

The theoretical calculations from the design model and the test data are both available to characterize the response of several of the control system components. Some parts of the system were designed from theory and could not be accurately analyzed experimentally. Other parts were copied from components with a known response and their actual response was then measured experimentally. An attempt is made here to compare, where possible, both experimental* and theoretical data, and in other cases to take the data available and compare it with the response that might be expected.

Temperature Sensor

Both theoretical and experimental data are available on the temperature sensor, as shown in Fig. 6. From this figure it can be seen that the actual response of the sensor is somewhat less than that predicted by the theory. This difference can be attributed to factors in both the theory and the experimental procedure.

Studying the theoretical calculations in Appendix II several assumptions are found which could have a notable effect on the sensitivity of the sensor. First, the assumption that the normalized force plot is symmetrical is not exact and can only be an approximation at best. Also,

---

*Complete experimental results are given in Appendix V.

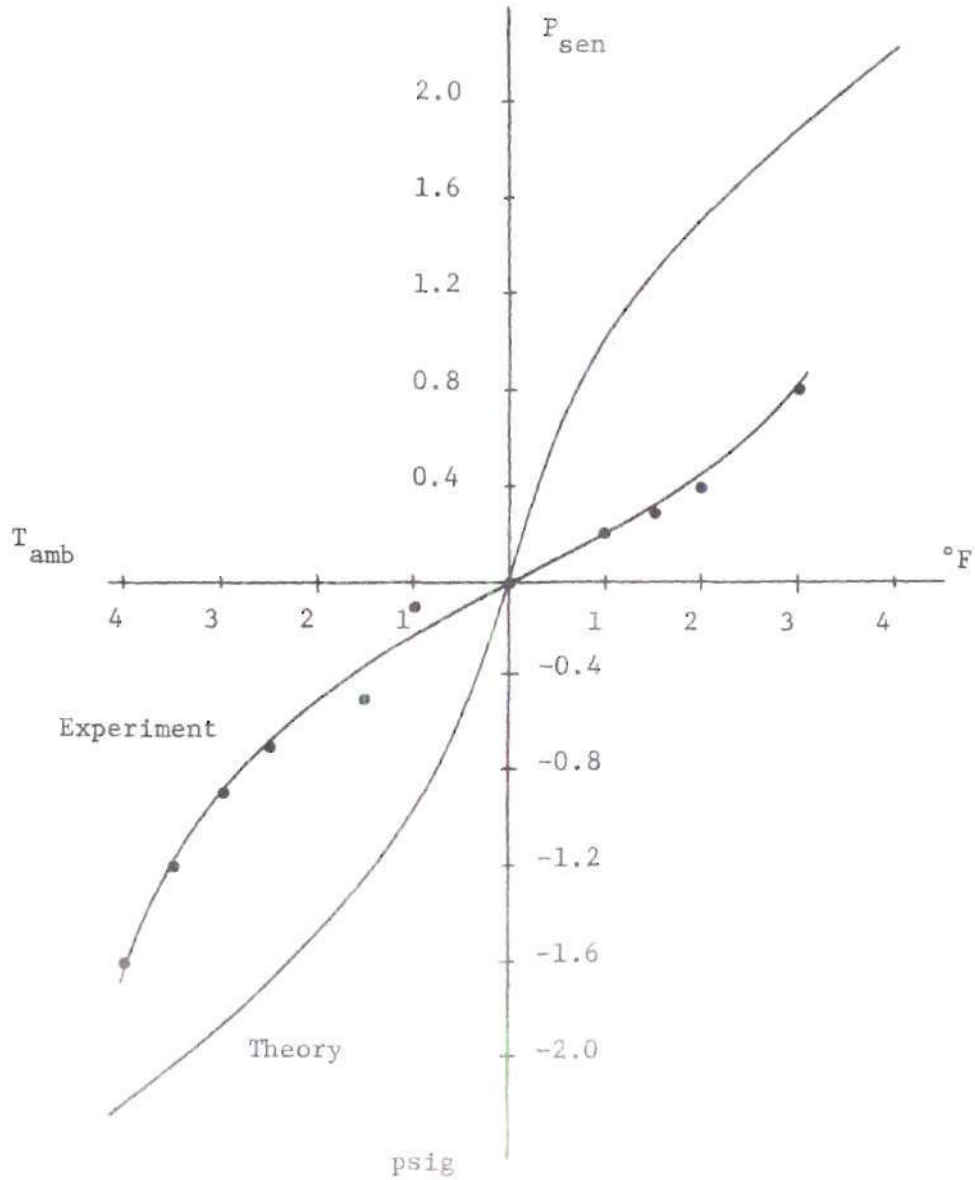

Figure 6. Open-loop Response of the Temperature Sensor

the values in this plot and several other calculations can be varied by a change in the assumed values of the orifice coefficients.

In the experimental model the accuracy in setting the nozzle separation is important. This distance is not easily measured and a variation of less than one-thousandth of an inch has an appreciable effect on the sensor output. Inaccuracies in centering the flapper would have similar effects on the output. Finally, not all of the points on the experimental response curve are steady-state points. This would cause the pressure response to be low because of the time lag of the bimetal, as explained below.

The time response of the sensor pressure to temperature changes is approximately a first order lag with a time constant of about 1/2 minute for a temperature change of 2°F. The theory assumes that the bimetal is at the ambient temperature, but actually it requires a finite time for the mass of the bimetal, which was kept near the minimum, to changes its temperature. Thus the heating or cooling of the bimetal is the main factor in the time response of the sensor.

Pressure Amplifiers

The theoretical response of the pressure amplifiers is taken from the manufacturer's curves (see Figs. 7, 8). These curves give the typical gains and operating points for both the proportional and center dump amplifiers. The output bias pressure cannot be determined from these curves, however, only the differential output pressure can be found.

The actual response of the pressure amplifiers was found by cross-plotting data from Tests B and C. The resulting curve is shown in Fig. 9.

This curve is not especially accurate simply because it is a combination of data from two different tests, but it does give a good indication of the type of response that is obtained. The fact that this graph does not pass through the origin is partly due to fluctuations in supply pressure, accuracy in pressure measurement, and slight geometrical asymmetries in the amplifiers.

Comparing the manufacturer's data and the experimental data it can be seen that the actual gain reaches about four while the theoretical gain at the operating pressure of about three psig, which was used, was about five. The Corning units are designed for a supply pressure of five psig and for loads of 0.98 and 0.84 times the receiver areas for the proportional and center dump amplifiers, respectively. The supply pressure actually used was ten psig. This difference will certainly affect the gain, but it was assumed to be a small error. The impedance matching error was a greater problem, however. Due to an error in some preliminary design calculations, the input impedance of the flow amplifier was made less than the output impedance of the Corning amplifier. This mismatch caused a lower overall pressure gain than might otherwise have been expected. The lower pressure gain may have been partially counteracted, however, by a slight increase in output flow from the second stage because of the lower impedance in the following stage, the flow amplifier.

Flow Amplifier, Controllers, and Air Mixer

The flow amplifier, controllers, and air mixer were lumped as one component experimentally because of difficulties in flow measurement. To avoid the use of the flow parameter, this lumped component is characterized by the pressure differential input to the flow amplifier

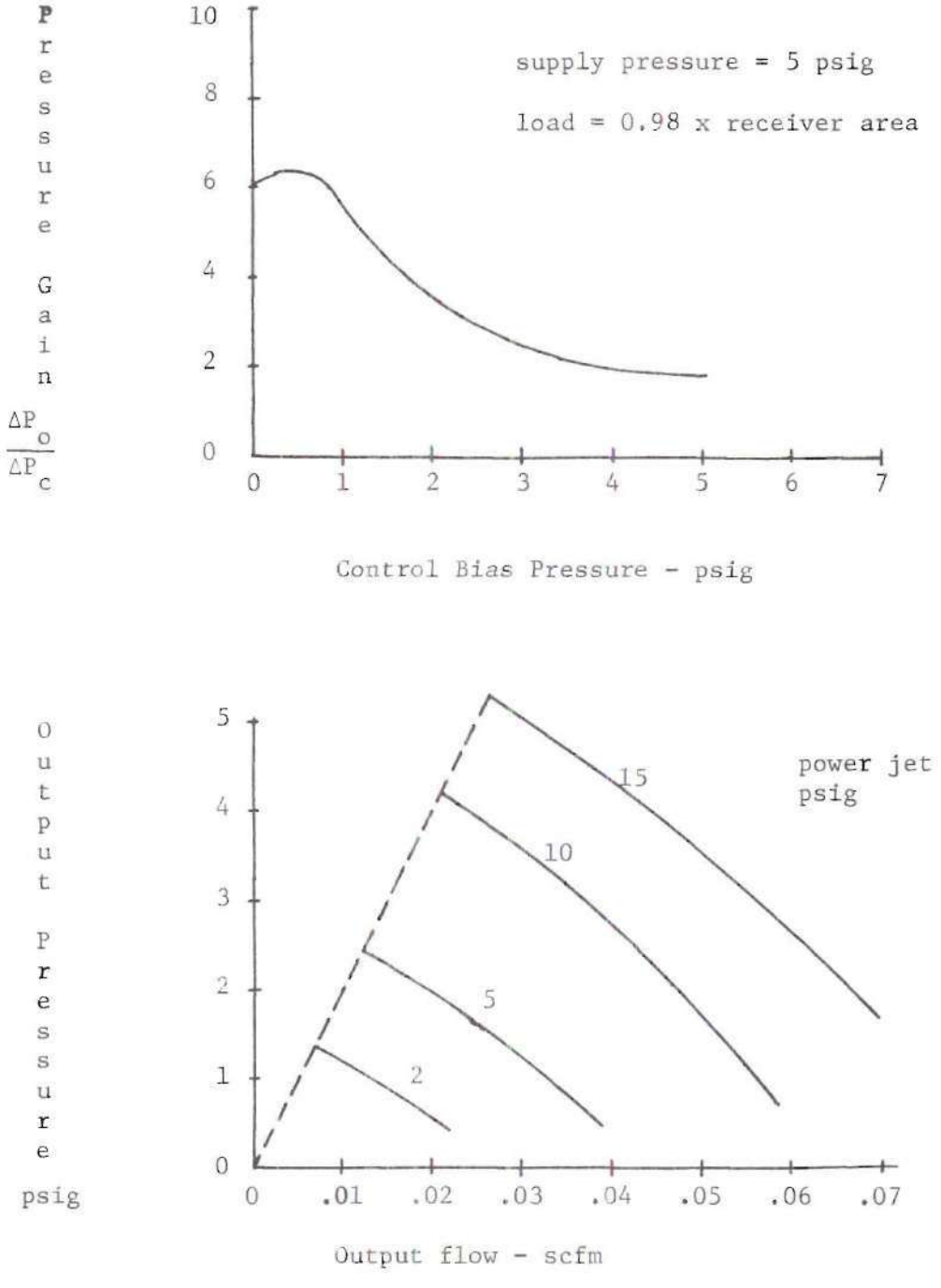

Figure 7. Typical Gain and Output Characteristics of the Corning Fluidic Proportional Amplifier.

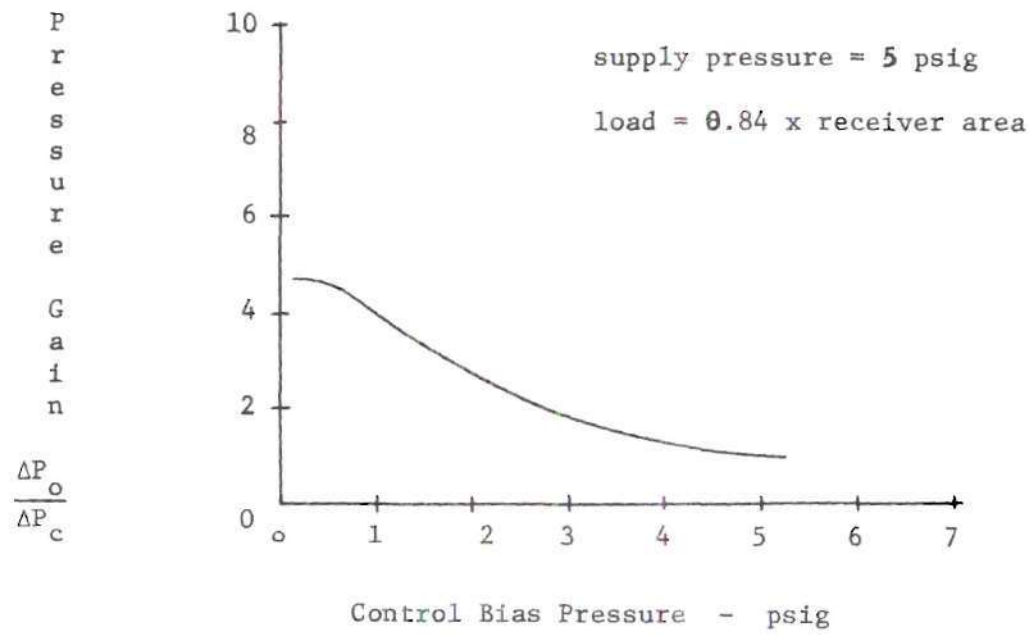

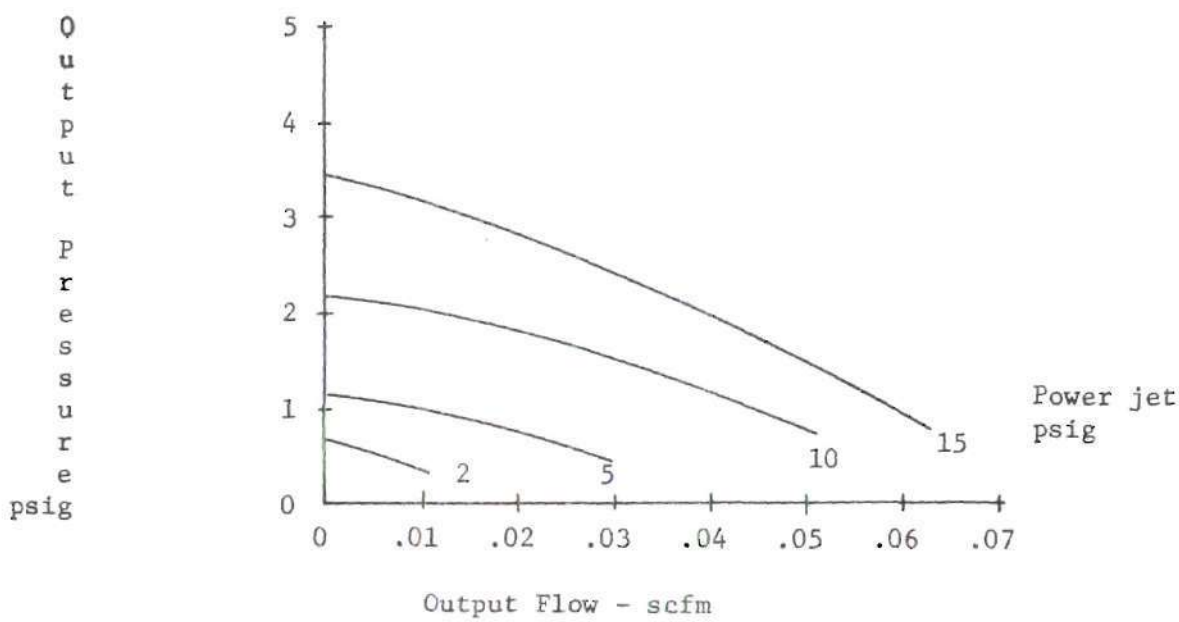

Figure 8. Typical Gain and Output Characteristics of the Corning Fluidic Center Dump Proportional Amplifier

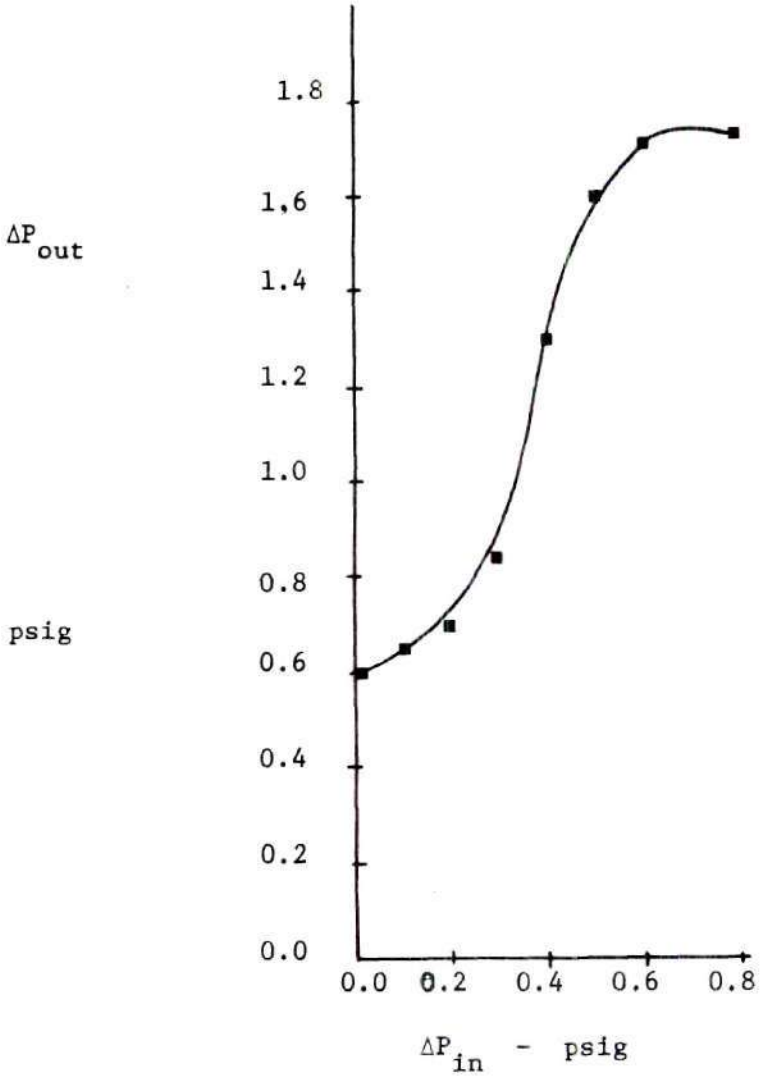

Figure 9. Open-loop Response of Pressure Amplifiers (two stages)
(two stages)

and the output temperature of the mixer. The actual response of this "black box" is shown in figure 10.

The theoretical response of this lumped component is not available because the temperature levels in the Hilsch tube, proportional controllers, and mixing tube could not be determined analytically.

The fabrication and design problems previously noted in properly sizing the channels in the controllers again caused impedance mismatching. This lowered the flow gain of the proportionals and the final result was a narrower output temperature range than might have been expected. A temperature range of at least 30°F was expected, but the actual range is in the vicinity of 20°F.

The time response of the temperature is determined mainly by the time it takes for the temperature of the controller to reach steady-state. This time lag is greatest at start-up, as might be expected, because the temperature change is the greatest. At least fifteen minutes is usually required after start-up before the steady-state temperature is reached. This also includes the response time of the Hilsch tube, however. After the initial steady-state is attained, the Hilsch tube temperature does not change. At this point the temperature response to a change in input pressure requires less than one minute, regardless of the size of the temperature change.

The input-output curve in figure 10 indicates that the hot temperature range is small. This response is due to the sensor response previously noted. Other factors that could contribute to an unbalanced response might be excessive dilution of the hot air by the control air, or slight asymmeteries in the amplifier construction.

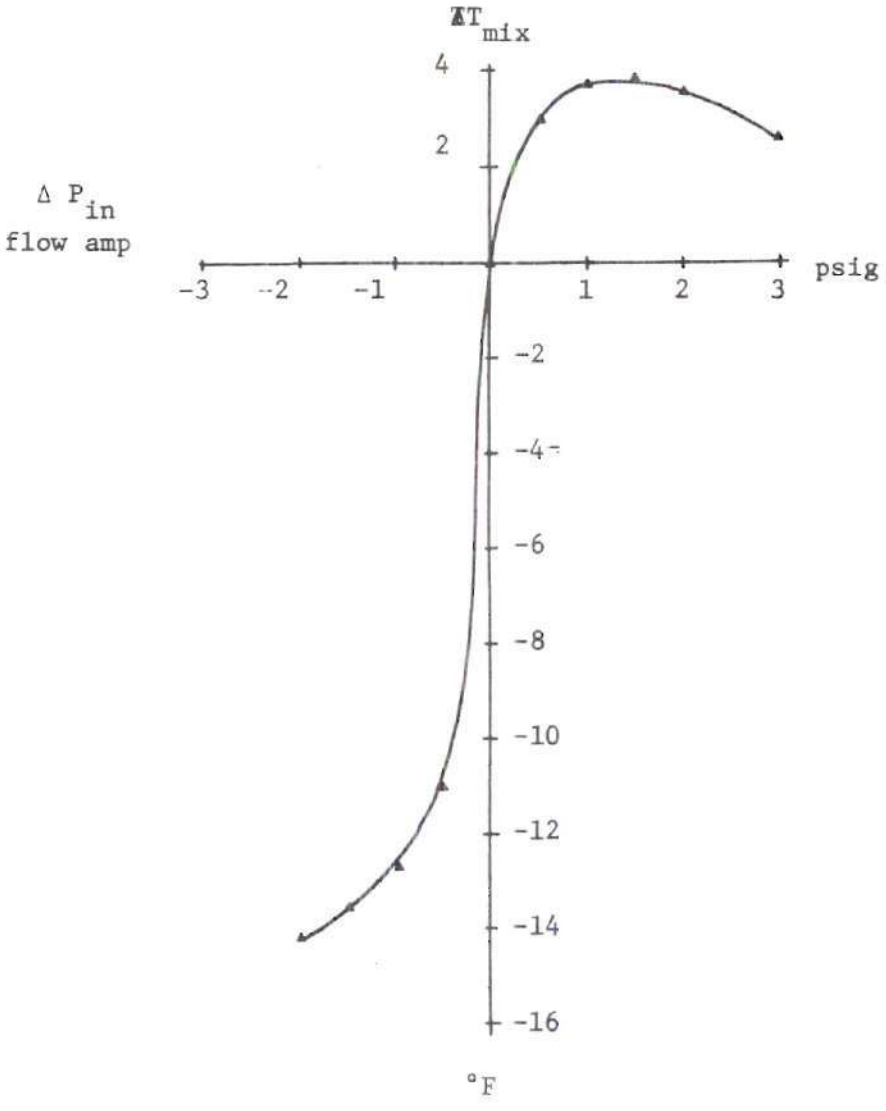

Figure 10. Open-loop Response of the Flow Amplifier, Control Amplifiers, and mixing tube

Hilsch Tube

M. P. Blaber (13), in his data on a modified Hilsch tube from which the one for this system was copied, states that at about 60 psig his tube could be set for a maximum temperature of 190°F or a minimum temperature of -5°F. If the hot and cold output flows are balanced at the same input pressure of 60 psig, the temperature extremes are 142°F and 12°F.

The Hilsch tube built for this project had very nearly the same dimensions as Blabers's. It was operated at 40 psig, a limit set by the capacity of the air system available. The limits on the temperature extremes were found to be 146°F and 9°F at 40 psig. For approximately equal output flows, the temperature range is 130°F on the hot side and 32°F on the cold side. Naturally these temperatures are attenuated as the air travels through the system.

Temperature Controlled Container

The equations expressing the theoretical heat balance in the temperature controlled box are shown in Appendix IV. There are an infinite number of operating conditions which could be substituted into these equations and a response obtained for each one.

Experimental thermal data from the previously described tests are available for the system. These data are not readily adaptable to the theoretical equations to solve for the flow because the air flow through the box was not controlled at a constant value for the two conditions, with and without the heater. This condition is required if $\dot{m}$ is to be found by simultaneous solution of the two heat balances.

The open-loop temperature response of the box with no external heat source (lamp) adding heat to the system is shown in Fig. 11. The

drop of ΔT_{amb} at $\Delta T_{mix} = 4°$ was caused by the limited response of the sensor, as described. Over most of the range the response appears to be linear.

The time response of the box can also be seen from the graphs of Tests A and B, pp 66-74. For small changes in input temperature the ambient temperature responded in less than one minute (the smallest time increment measured). For input changes of 8-10°F, as on start-up, the box required 10-12 minutes to reach a new steady-state condition.

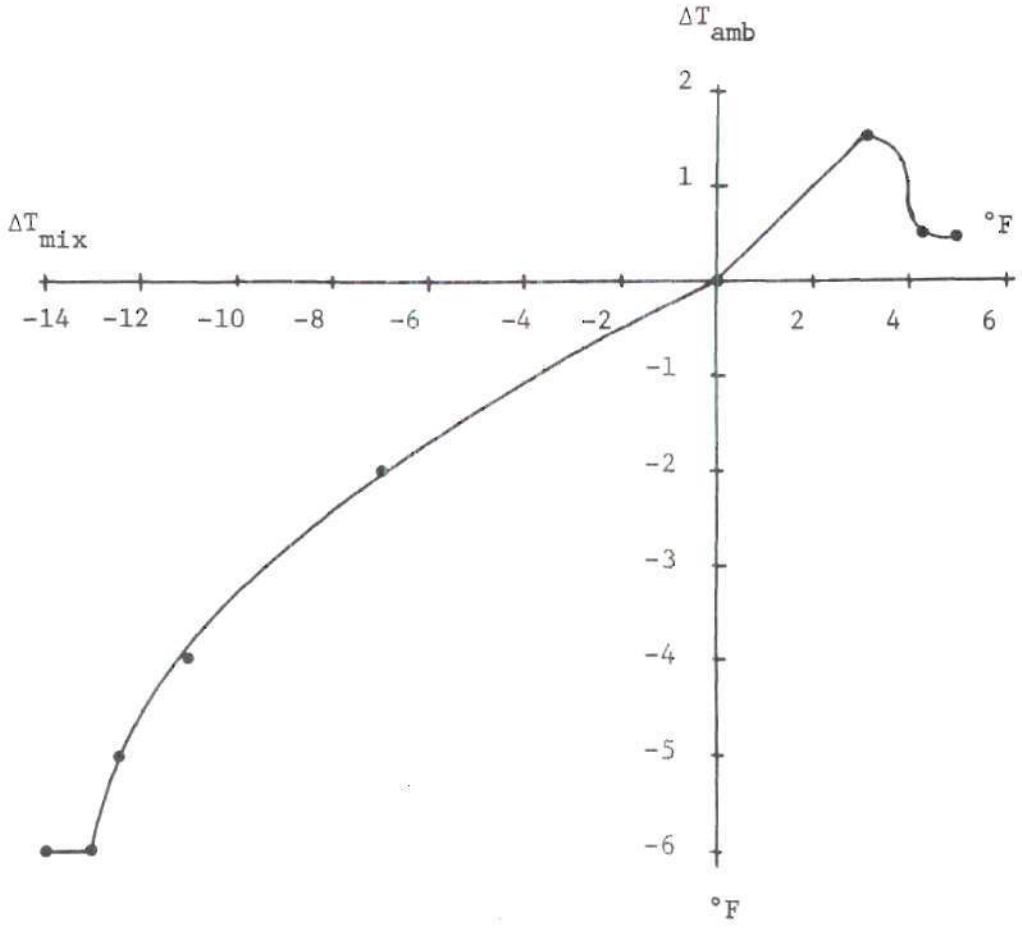

Figure 11. Open-loop Temperature Response of box

CHAPTER VI

CONCLUSIONS

From the data comparison in the previous chapter and first-hand experience in the design and operation of the temperature control system, several basic conclusions may be drawn:

1. The total system is inefficient and, without further improvement, can only be practical where a large supply of compressed air is inexpensively available.
2. The system is highly reliable and requies no operator attention after it is initially adjusted and set into operation.
3. The entire system operates off of a single air supply and requires no auxiliary power supplies of any sort.
4. The only energy interfaces in the system are between temperature and pressure.
5. The temperature sensor is quite accurate and its time response, though not considered rapid, is fast enough for this and most applications. It could be a useful control element in other fluidic systems.
6. The pressure amplifiers operate well, although their actual gains could have been improved by closer matching of impedances.
7. The gain and response of the flow and control amplifiers are very low and could have been improved significantly by better impedeance matching.

8. The Hilsch tube, in spite of its inherent inefficiency has potential in the field of pure-fluid devices when utilized for both its heating and cooling capabilities.

CHAPTER VII

RECOMMENDATIONS

The two recommendations that would effect the greatest improvements in this system are increasing the gain of the fluidic amplifiers, and the thermal efficiency of the system.

The entire response of this system could be enhanced by the use of more precisely constructed fluidic amplifiers. These could be either commercial units of the proper size, as indicated in Appendix III, or ones constructed in the laboratory by optical milling or other sophisticated techniques. The ones constructed for this project were not exactly symmetrical, and some difficulty was encountered in constructing the small passages required.

The thermal efficiency of the system could be increased by improving the efficiency of the Hilsch tube and by insulating the components and lines carrying hot and cold air. The Hilsch tube may be made more efficient by using a spiral vortex instead of a circular one. If a commercially manufactured or carefully machined vortex tube could be obtained, the difference in the hot and cold air temperatures could be significantly increased. These extreme temperatures could be maintained longer if some care were taken to insulate the system with asbestos or other thermal insulating material and shorten all tubing as much as possible. The temperature change across the controllers could be reduced by constructing the elements from plastic or glass. Also, some

of the thermal losses are due to the mixing of the room temperature control air with the high and low temperature air. This effect could be minimized by designing the proportional controllers for as high a flow gain as possible. Little care was taken with regard to thermal insulation because the initial and foremost object was the response and feasibility, rather than the range, or the control system.

Finally, a few comments concerning the air supply might be helpful in future endeavors. The air supply used for this experiment could not be operated for more than 14-20 minutes before the supply pressure dropped below the 40 psig required to operate the Hilsch tube. This Hilsch tube and control system requires roughly four to six standard cubic feet per minute of flow at a minimum of 40 psig for as long as it is intended to operate. In addition, the air should be clean and dry.

APPENDIX I

BIMETAL DESIGN

For a spiral bimetal as shown in Figure 12 the deflection equation is:

$$x = - \frac{LK_{DC}mr\Delta T}{57.3\ t} \qquad (1)$$

and the load equation is:

$$F_T = \frac{K_{DC}K_{PC}b\ t^2(1 - m)\Delta T}{16\ r} \qquad (2)$$

where

K_{DC} = coil deflection constant in 1/°F.

K_{PC} = coil torque constant in oz/in^2.

t = thickness of bimetal in inches

b = width of bimetal in inches

r = radius to point of load application in inches

m = specific deflection $(D_f - D_l)/D_f$

D_f = free thermal deflection in inches

D_l = deflection caused by opposing load, in inches

ΔT = temperature change in °F

x = deflection of bimetal in inches

F_T = load in pounds

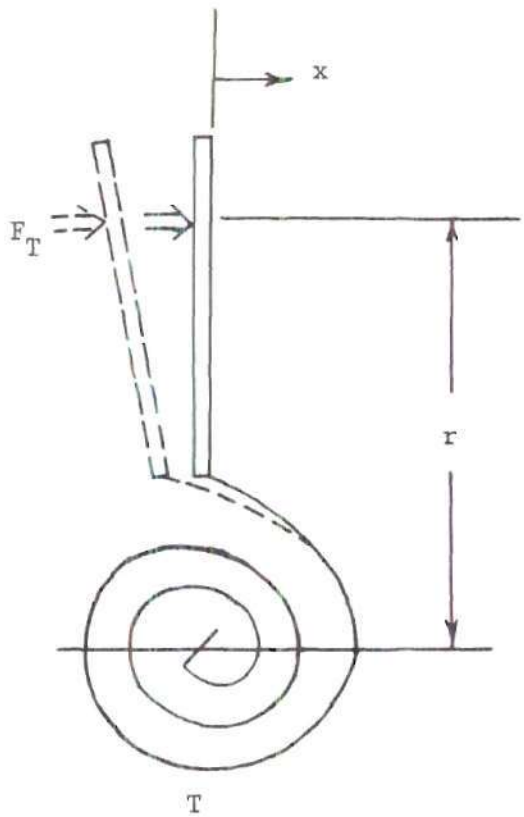

Figure 12. Bimetal Showing Sign Convention and Deflection for an Increase in Temperature

For Chace type 2400 thermostatic bimetal:

$K_{DC} = 9.5 \times 10^{-4}/°F$

$K_{PC} = 5.8 \times 10^{5}$ oz/in^2.

$t = 0.015$ in.

Values selected for other parameters:

$b = 0.250$ in.

$r = 1.00$ in.

$m = 0.67$ (assumed for calculation of L)

$x = 0.10$ in. maximum deflection

$\Delta T = 30°F.$ required to produce 0.10 in. deflection

Calculating the length of bimetal required (sign convention may be neglected here):

$$L = \frac{57.3\ tx}{K_{DC} mr\ \Delta T}$$

$$L = \frac{(57.3)(0.015)(0.10)}{(9.5 \times 10^{-4})(0.67)(1.00)(30)}$$

$$L = 4.5 \text{ inches}$$

APPENDIX II

SENSOR DESIGN

From Figure 13 the following flow relationships may be observed:

$$\dot{M}_{A1} = \dot{M}_{A2} + \dot{M}_{A3} \tag{3}$$

$$\dot{M}_{B1} = \dot{M}_{B2} + \dot{M}_{B3} \tag{4}$$

$\dot{M}_1$ is the flow through an orifice and may be expressed by the equation

$$\dot{M}_1 = \frac{A_1 C_d P_s}{T} \left\{ \frac{2Kg}{(K-1)R} \left[\left(\frac{P}{P_s} \right)^{2/K} - \left(\frac{P}{P_s} \right)^{(K+1)/K} \right] \right\}^{1/2} \tag{5}$$

$\dot{M}_2$ is the flow through an orifice operated as a flapper valve and may be expressed by

$$\dot{M}_2 = \frac{C_f \pi P d \, (L/2 \pm x)}{T} \left\{ \frac{2Kg}{(K-1)R} \left[\left(\frac{P_a}{P} \right)^{2/K} - \left(\frac{P_a}{P} \right)^{(K+1)/K} \right] \right\}^{1/2} \tag{6}$$

The plus sign is for $\dot{M}_{A2}$ and the minus sign is for $\dot{M}_{B2}$.

$\dot{M}_3$ is the control flow and it also flows through an orifice which is actually the control port on the first stage amplifier. This flow may also be expressed by an orifice flow equation of the same form as $\dot{M}_1$.

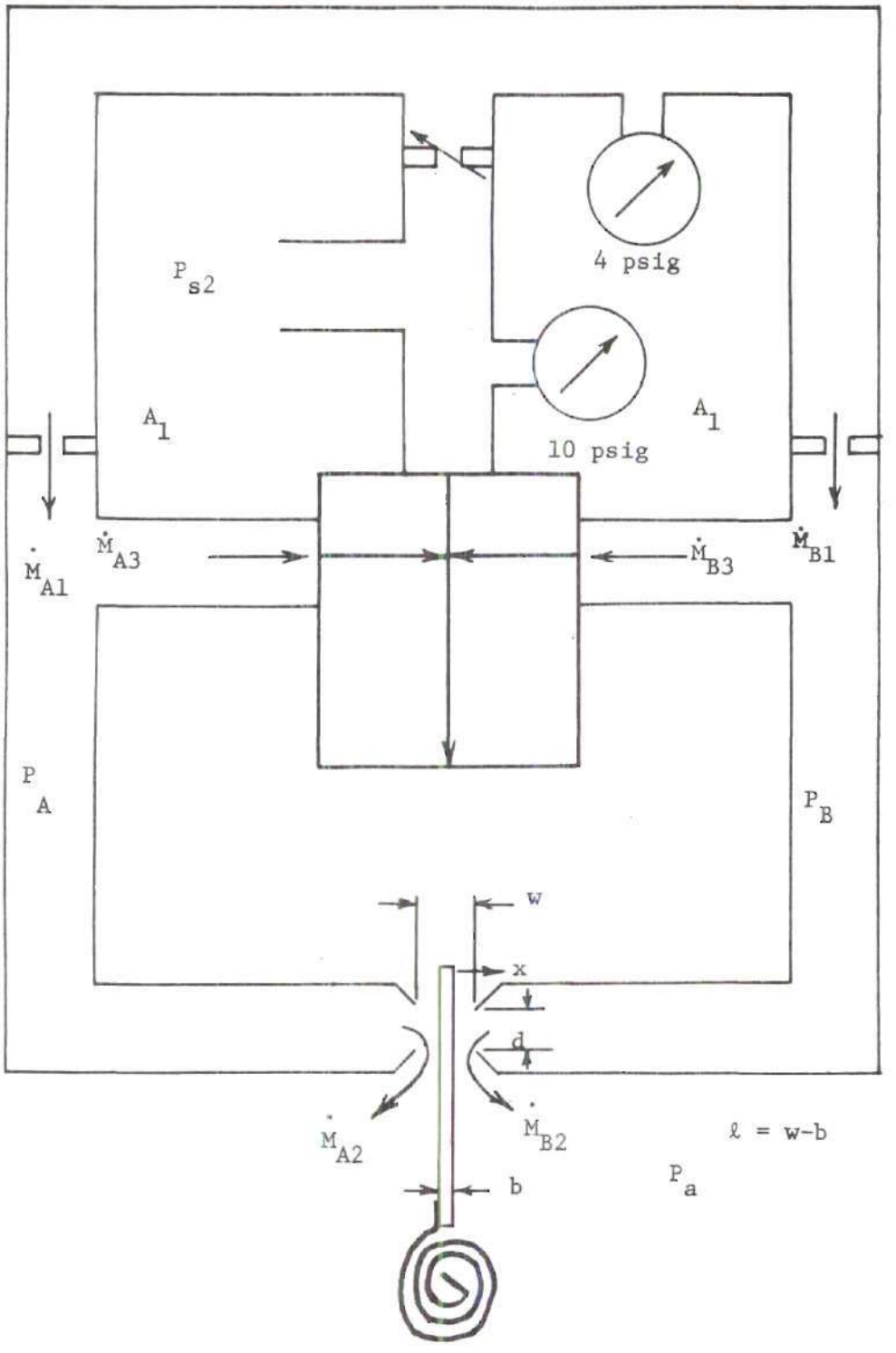

Figure 13. Temperature Sensor Schematic with Notation

$$\dot{M}_3 = \frac{A_2 C_d P}{T} \left\{ \frac{2KG}{(K-1)R} \left[\left(\frac{P_1}{P} \right)^{2/K} - \left(\frac{P_1}{P} \right)^{(K+1)/K} \right] \right\}^{1/2} \tag{7}$$

Substituting equation (5), (6), and (7) into (3) and (4) and factoring out the constant

$$\left(\frac{2KG}{(K-1)RT} \right)^{1/2}$$

Gives two equations

$$A_1 C_d P_s \left[\left[\left(\frac{P_A}{P_s} \right)^{2/K} - \left(\frac{P_A}{P_s} \right)^{(K+1)/K} \right]^{1/2} \right] =$$

$$C_f \pi d P_A (L/2 + x) \left[\left(\frac{P_a}{P_A} \right)^{2/K} - \left(\frac{P_a}{P_A} \right)^{(K+1)/K} \right]^{1/2} + \tag{8}$$

$$A_2 C_d P_a \left[\left(\frac{P_{A1}}{P_A} \right)^{2/K} - \left(\frac{P_{A1}}{P_A} \right)^{(K+1)/K} \right]^{1/2}$$

$$A_1 C_d P_s \left[\left(\frac{P_B}{P_s} \right)^{2/K} - \left(\frac{P_B}{P_s} \right)^{(K+1)/K} \right]^{1/2} =$$

$$C_f \pi d P_B (L/2 - x) \left[\left(\frac{P_a}{P_B} \right)^{2/K} - \left(\frac{P_a}{P_B} \right)^{(K+1)/K} \right]^{1/2} + \tag{9}$$

$$A_2 C_d P_B \left[\left(\frac{P_{B1}}{P_B} \right)^{2/K} - \left(\frac{P_{B1}}{P_B} \right)^{(K+1)/K} \right]^{1/2}$$

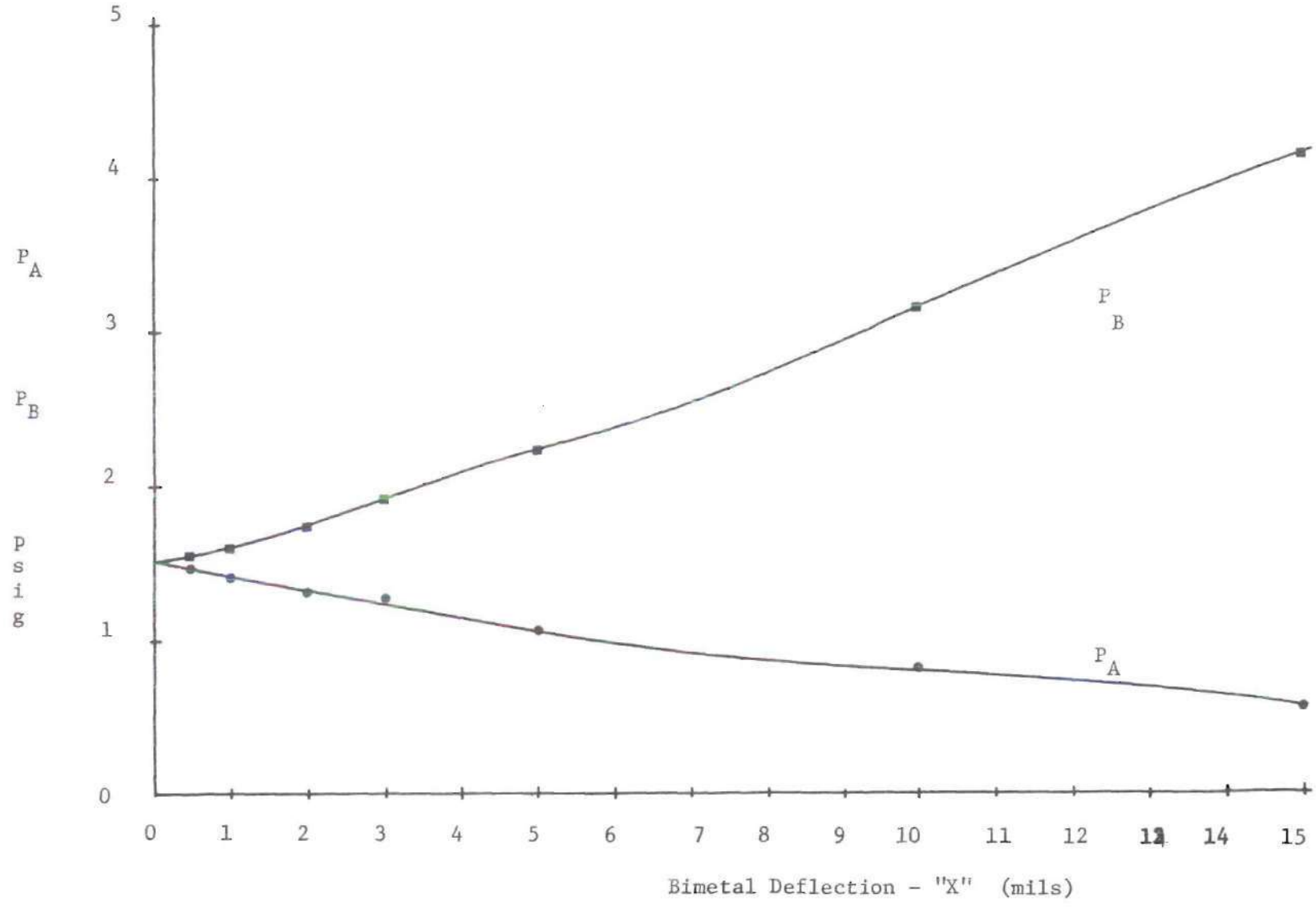

Figure 14. Solution of Flow Equations

These equations are solved for P_A and P_B in terms of x in Fig. 14. The values selected for the constants are:

P_s = 4.5 psig = 19.2 psia

P_a = 14.7 psia

P_1 = 14.7 psia

C_d = 0.8

C_f = 0.6

L = 0.03125 in.

d = 0.040 in.

$A_1 = (\pi/4)(0.40)^2 = 1.258 \times 10^{-3}$ in^2.

$A_2 = (0.015)(0.025) = 3.75 \times 10^{-4}$ in^2.

In addition to the mass flow balance in the nozzles, a force balance must also be made on the bimetal lever. From Blackburn (10) the air flow-forces on a plate from a nozzle can be expressed by equation (10).

$$F = \pi r^2 P \left[1 + \left(\frac{2C_d x}{r} \right)^2 \right] \tag{10}$$

where

r = radius of nozzle orifice

P = pressure upstream of orifice

C_d = orifice coefficient

x = separation between nozzle and plate

Substituting in the notation of the sensor diagram, Fig. 13, the forces on either side of the bimetal lever are

$$F_A = \frac{\pi d^2 P_A}{4} \left\{ 1 + \left[\frac{4C_d (L/2 + x)}{d} \right]^2 \right\} \tag{11}$$

$$F_B = \frac{\pi d^2 P_B}{4}\left\{1 + \left[\frac{4C_d(L/2 - x)}{d}\right]^2\right\} \qquad (12)$$

Equations (11) and (12) are valid only for small values of $2(L/2 \pm x)/d$. When this is no longer the case, the exact law of force is unknown, but a limiting value for large separations is reached when the quantity in the brackets reaches two, as explained by Blackburn (10). The equation for this limiting case is:

$$F = 2\pi r^2 C_c P \qquad (10A)$$

where the contraction coefficient C_c is nearly unity. Figure 15 is a plot of equations (10) and (10A). In order to make figure 15 a smooth curve, the portion of the normalized force above 1.5 is arbitrarily made symmetrical to the portion below 1.5. Then, to calculate the force of equation (10) values of the quantity in brackets are selected from the graph for corresponding values of the ratio $2(L/2 \pm x)/d$. Using the constants previously given, F_A and F_B are calculated in terms of x and plotted in Fig. 16. Values of P_A and P_B are found in Fig. 14 for corresponding values of displacement.

The total force balance on the bimetal lever is then

$$F_T = F_A - F_B \qquad (13)$$

where F_T is the force exerted by the bimetal. This force may be found by eliminating the unknown quantity m in the simultaneous solution of equations (1) and (2).

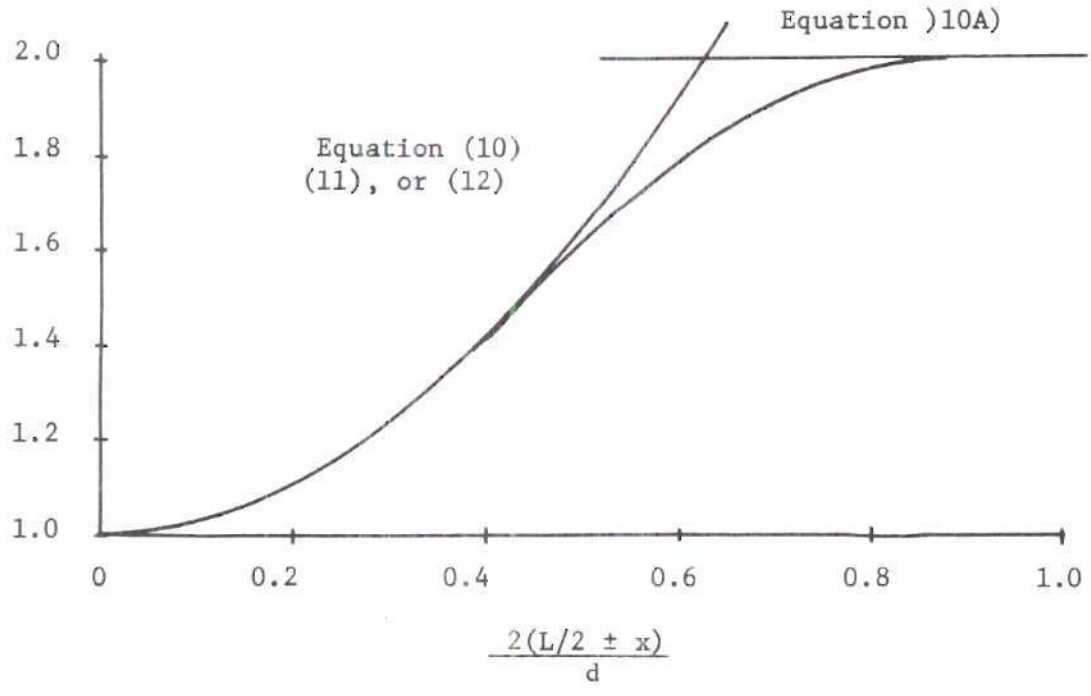

Figure 15. Normalized Solution of Flapper Force Equations

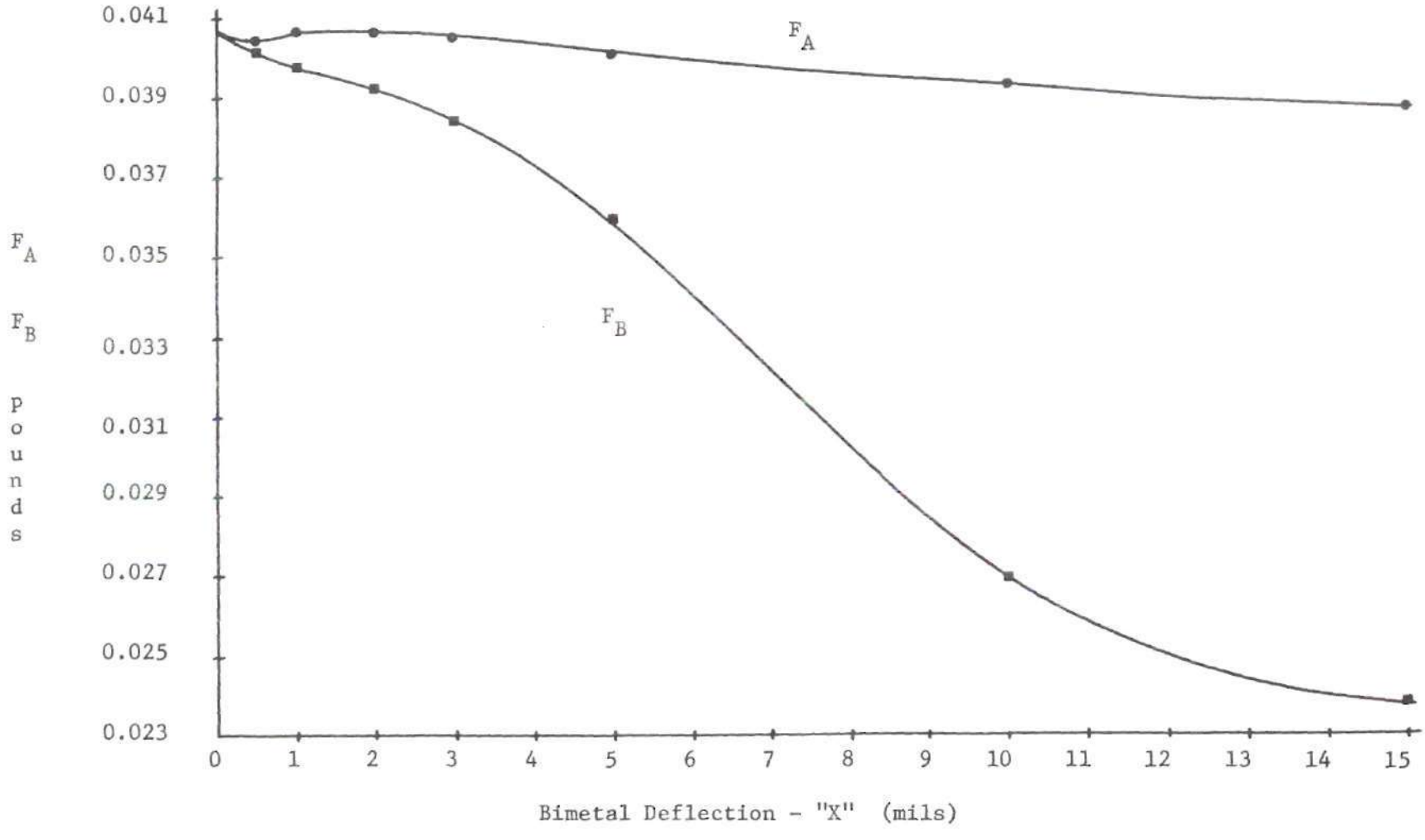

Figure 16. Solution of Equations of the Flow Forces Acting on the Bimetal Lever

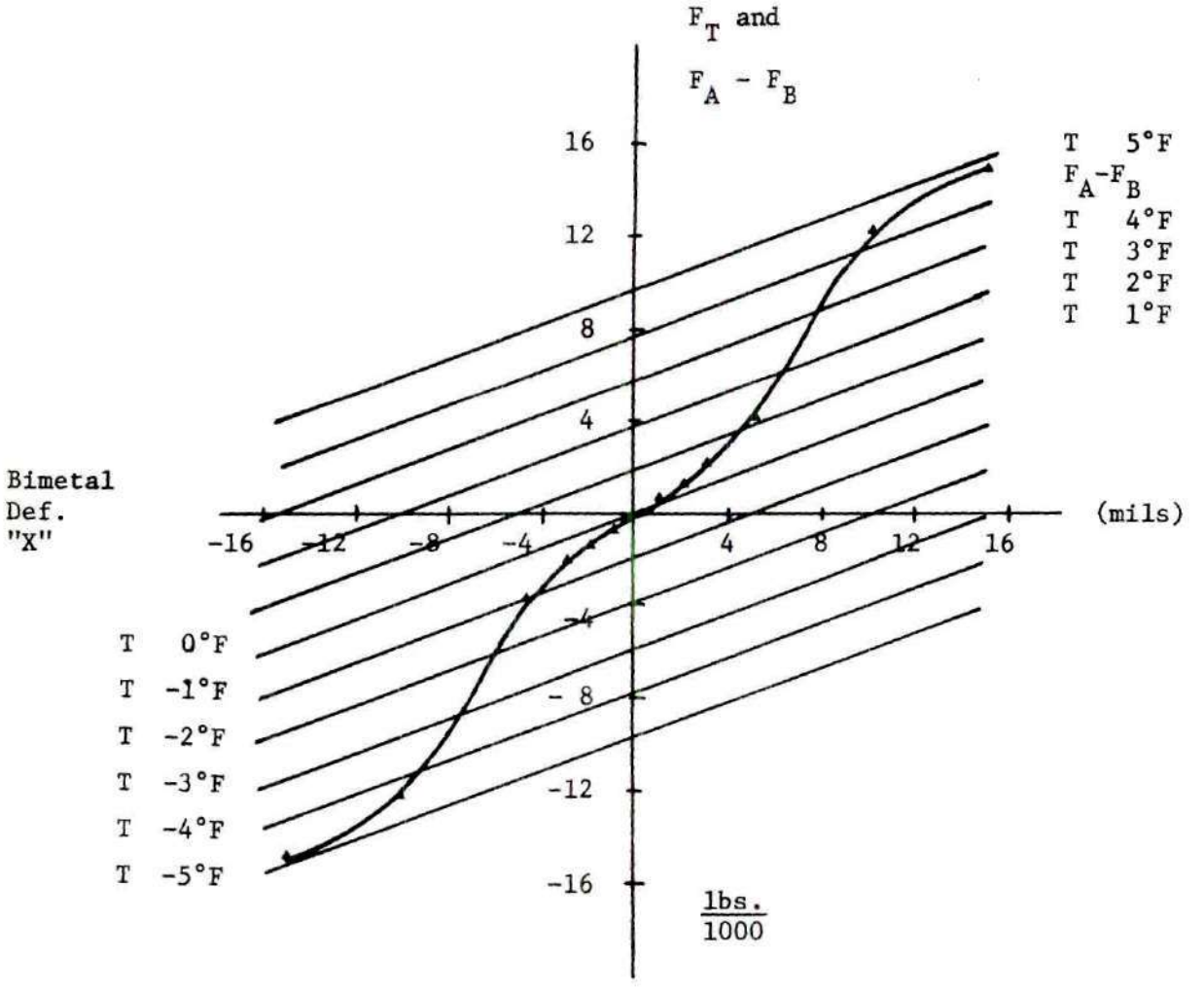

Figure 17. Solution of Force Balance Equation (13).

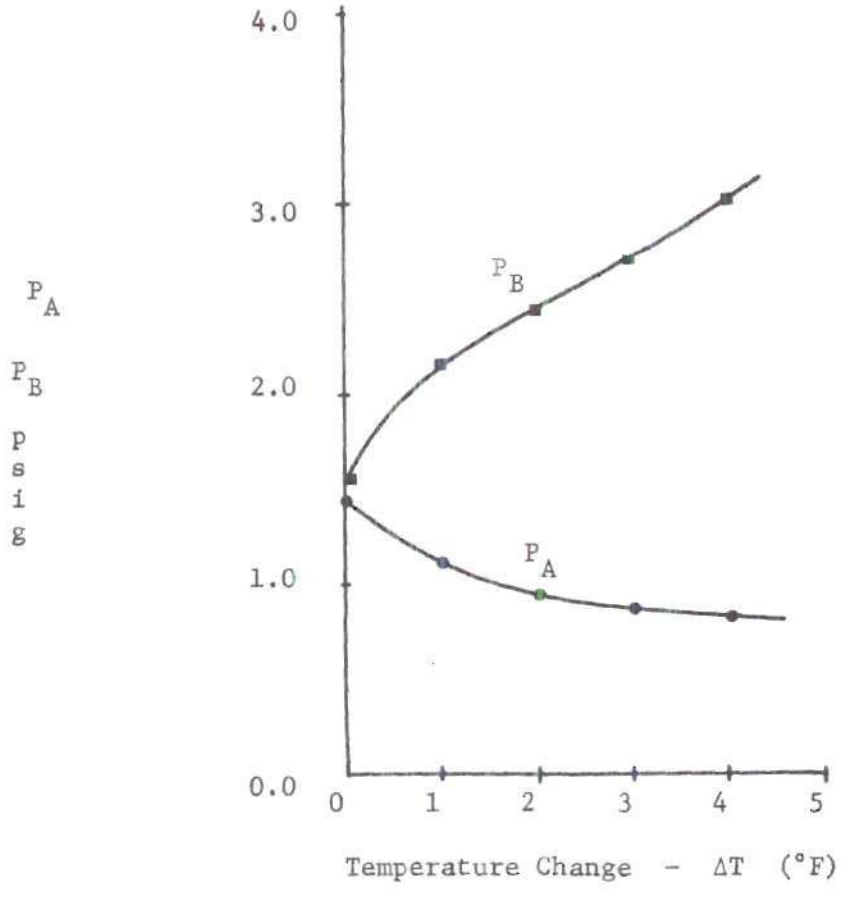

Figure 18. Temperature-Pressure Response of Sensor with Bimetal Initially Centered

$$m = -\frac{57.3tx}{K_{DC}Lr\ \Delta T} \tag{1}$$

$$m = 1 - \frac{16F_T r}{K_{DC}K_{PC}bt^2\ \Delta T} \tag{2}$$

Equating and solving for F_T

$$F_T = \frac{K_{PC}bt^2}{16r}\left[K_{DC}\Delta T + \frac{57.3tx}{rL}\right] \tag{14}$$

Using the constants previously given, F_T is solved graphically in terms of ΔT and x in figure 16.

The force balance of equation (13) may now be solved graphically. The difference, $F_A - F_B$, is determined from figure 16 for values of x and plotted on the graph of F_T versus x for constant values of ΔT. Each point of intersection on this graph is a solution of equation (13) for the proper values of x and ΔT. This may be converted to P_A and P_B as a function of ΔT only by finding from figure 14 the values of P_A and P_B at the corresponding values of x. The resulting plot of P_A and P_B versus ΔT is shown in figure 18. This curve represents the pressure response of the temperature sensor to a given thermal change.

APENDIX III

AMPLIFIER DESIGN

The flow and control amplifiers were both designed from models presented by E. M. Dexter (6), and by R. J. Reilly and F. A. Moynihan (7).

As shown in Dexter's model, from a geometrical standpoint the pressure gain of an amplifier is a maximum for a receiver located from five to nine nozzle widths from the power nozzle. If the receiver is made $1.5w_o$ wide and placed six nozzle widths from the power nozzle, then

$$\text{Tan } \theta_{max} = \left(\frac{1.5w_o}{2} \right) \left(\frac{1}{6w_o} \right)$$

and

$$\text{Tan } \theta_{max} = 0.125$$

$$\theta_{max} = 7.13°$$

Flow Amplifier

Also from Dexter's model

$$\text{Tan } \theta = \frac{w_c \Delta P_c}{w_o P_o} \tag{15}$$

and from Reilly's non-viscous flow model

$$\text{Tan } \theta = \frac{K}{k} \left(\frac{\Delta \dot{M}_c}{\dot{M}_o} \right) \tag{16}$$

From equation (15)

$$k = \frac{w_c}{w_o} = \text{Tan } \theta \left(\frac{P_o}{\Delta P_c} \right) \tag{17}$$

Substituting for K and solving equation (16) for $\dot{M}_o$

$$\dot{M}_o^2 = \frac{(\dot{m}_{cl} + \dot{m}_{cr})\ \Delta\dot{m}_c}{k \tan \theta_{max}}$$

Assume $\dot{m}_{cl} = \Delta\dot{m}_c = \dot{m}_{out}$ from the Corning amplifier, and $\dot{m}_{cr}$ is approximately zero

$$\dot{M}_o = \left[\frac{(\Delta\dot{m}_c)^2}{k \tan \theta_{max}} \right]^{1/2} \tag{18}$$

From the Corning amplifier characteristic curves the volumetric flow rate is approximately 0.04 ft^3/min. To calculate the mass flow, the air density must first be determined. Roughly

$$\rho = \frac{P}{RT}$$

and for $P = 24.7\ lb/in^2$

$T = 530°R$

$R = 53.35\ (ft\text{-}lb)/(lb_m - °R)$

then $\rho = 7.3 \times 10^{-5} lb/in^3$.

Now calculating $\Delta\dot{m}_c$

$$\Delta\dot{m}_c = \left(\frac{0.04\ ft^3}{min} \right) \left(\frac{7.3 \times 10^{-5} lb}{in^3} \right) \left(\frac{12\ in}{ft} \right)^3$$

$$\Delta\dot{m}_c = 5.05\text{x}10^{-3}\ \text{lb/min}$$

k is determined from equation (17) when P_o = 10 psig and $P_c \tilde{\sim}$ 6 psig. Then k = 0.208. Finally solving equation (18) for $\dot{M}_o$ of the flow amplifier: $\dot{M}_o = 3.13\text{x}10^{-2}$ lb/min = $5.22\text{x}10^{-4}$ lb/sec.

The area, A_1, of the power orifice is calculated from compressible flow equations presented by Blaine W. Andersen's The Analysis and Design of Pneumatic Systems, equation (2.1-15).

$$A_1 = \frac{\dot{M}_o \quad T}{K' P_o N_{12}} \tag{20}$$

For a pressure differential of 10 psig, P_o/P_a = 24.7/14.7 = 1.68, and the corresponding values of K' and N_{12} are 0.180 and 0.990, respectively, from Andersen's tables. Using a temperature of about 530°R, the area, A_1, of the power orifice of the flow amplifier is calculated to be $2.72\text{x}10^{-3}$ in^2.

For an aspect ratio of two,

$$A_1 = 2w_o^2 \tag{21}$$

or

$$w_o = \sqrt{\frac{A_1}{2}}$$

$$w_o = 3.69\text{x}10^{-2}\text{in}$$

and

$$D = 2w_o = 7.38\times10^{-2}\text{in}$$

$$w_c = 0.208w_o = 7.67\times10^{-3}\text{in} \tag{21a}$$

To calculate the output flow of the flow amplifier Reilly presents the following equation:

$$\Delta\dot{M}_{out} = 2M_o \frac{L}{w_o} \sin\theta - \Delta\dot{m}_c \tag{22}$$

For full jet deflection, when $\dot{M}_o = 3.13\times10^{-2}$ lb/min, $\Delta\dot{m}_c$ 5.05×10^{-3} lb/min, $L/w_o = 6$, $\sin\theta_{max} = 0.124$, $\Delta\dot{M}_{out} = 4.14\times10^{-2}$ lb/min.

The output to the flow amplifier is divided to drive the two controllers. Thus, $\Delta\dot{m}_c$ for the controllers is one-half of $\Delta\dot{M}_{out}$, or 2.07×10^{-2} lb/min.

Impedance Matching

In order to match the impedance seen by cascaded amplifiers, the outlet area of the first amplifier should be about the same as the total inlet area of the amplifier(s) immediately following. From figure 19

$$A_3 = 1.5A_1 \tag{23}$$

and matching orifice areas

$$A_3 = 2A_3' \tag{24}$$

then

$$A_3' = 0.75A_1 \tag{25}$$

Substituting in the value of A_1 previously found:

$$A_3' = 2.04\text{x}10^{-3}\text{in}^2$$

A_2 can also be determined as

$$A_2 = kA_1 \tag{26}$$

$$A_2 = (0.208)(2.72\text{x}10^{-3})$$

$$A_2 = 5.66\text{x}10^{-4}\text{in}^2$$

or $$w_2 = 7.67\text{x}10^{-3}\text{in.}$$

The actual dimensions of the flow amplifier are shown in Figure 21.

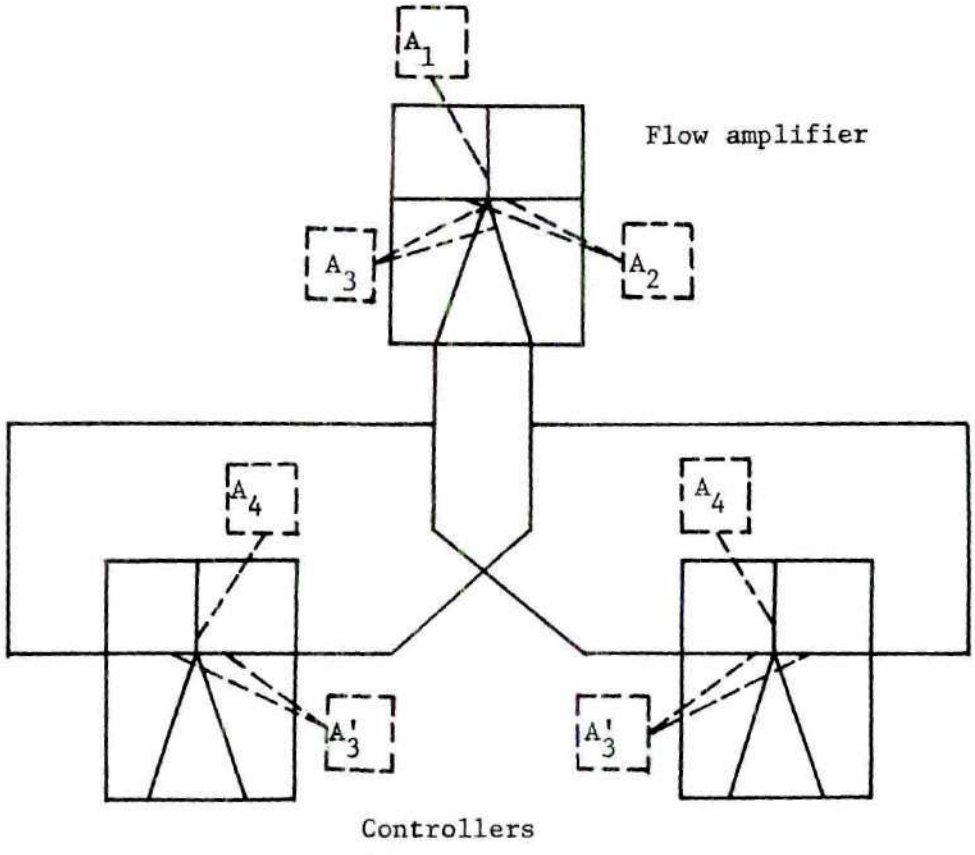

Figure 19. Impedance Area Designations for Amplifiers

Controllers

The required mass air flow through the power orifices of the controllers can be calculated from equation (18)

$$\dot{M}_o^2 = \frac{(\Delta\dot{m}_c)^2}{k \tan \theta_{max}} \tag{18}$$

The value of $\Delta\dot{m}_c = \Delta\dot{M}_{out}/2$ was found to be $2.07\text{x}10^{-2}$ lb/min, and the same value of θ is selected for the controllers as was used in the flow amplifier; therefore, $\tan \theta_{max} = 0.125$. Since the value of k is dependent on the flow or area and neither is known, a reasonable value of $k \simeq 0.2$ is selected. This will give a good gain and make it possible to calculate the required flow and orifice area. The required flow may be obtained by adjusting the hot and cold air bleed valves. Calculating the flow: $\dot{M}_o = 0.293$lb/min $= 4.89\text{x}10^{-3}$lb/sec.

The area of the power orifice of the controllers can now be calculated using equation (20). For a pressure differential of about 2 psig, the pressure ratio becomes

$$\frac{P_o}{P_a} = \frac{16.7}{14.7} = 1.137$$

For this pressure ratio, the values of K' and N_{12} are 3.109 and 0.669, respectively, from Andersen's tables. Although the temperature is different for the two controllers, an average value is selected as 530°R. Substituting these values into equation (20):

$$A_4 = \frac{\dot{M}_o \sqrt{T}}{K' P_o N_{12}} \tag{20}$$

$$A_4 = 3.24 \times 10^{-3} \text{ in}^2.$$

For an aspect ratio of 2, the power orifice dimensions may be calculated from equations (21) and (21a)

$$w_o = \sqrt{\frac{A_4}{2}} \tag{21}$$

$$w_o = 0.0403 \text{ in.}$$

$$D = 2w_o = 0.0805 \text{ in.} \tag{21a}$$

For this value of D, the width of the control orifices may now be determined:

$$w_c = \frac{A_3'}{D} \tag{27}$$

$$w_c = \frac{2.04 \times 10^{-3}}{8.05 \times 10^{-2}}$$

$$w_c = 0.0254 \text{ in.}$$

The actual construction dimensions of the controller are shown in Figure 20.

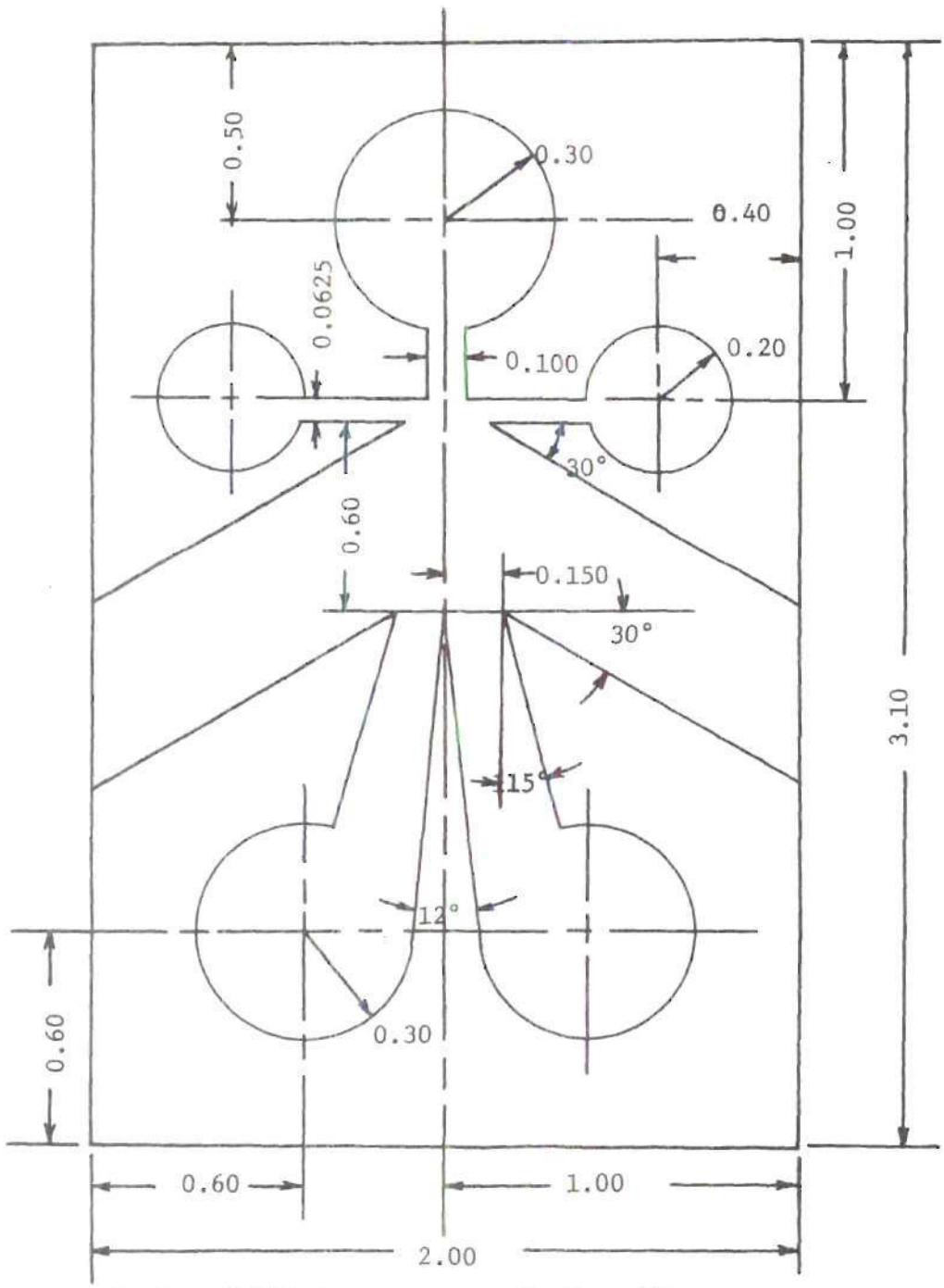

Figure 20. Proportional Controller (2 each)

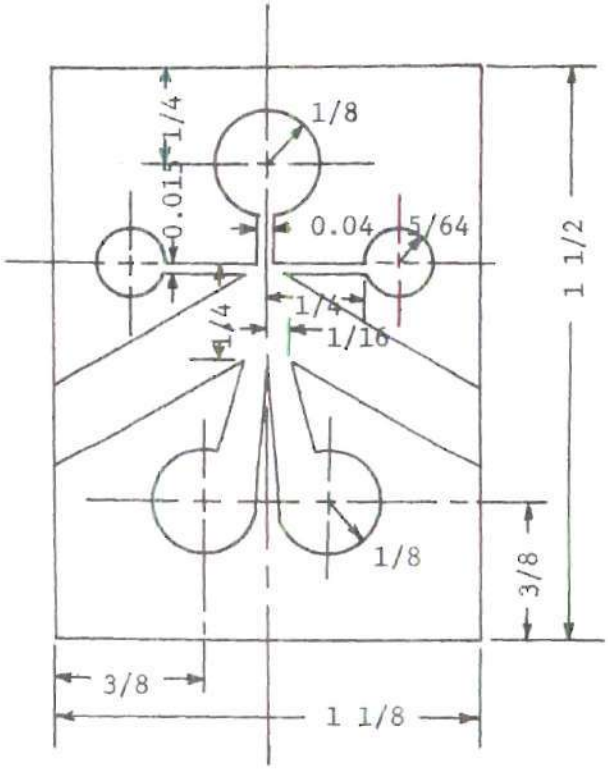

Depth - 0.094 in.
Scale - 2X
All angles same as in previous figure.

Figure 21. Flow Amplifier

APPENDIX IV

HEAT BALANCE EQUATIONS FOR THE TEMPERATURE CONTROLLED BOX

The balance for the temperature controlled box can be written for two different conditions: with and without an active heat source in the box.

When the heater is off

$$Q_{cool} = Q_{out} + Q_{lost} \tag{28}$$

or

$$c_p m(T_m - T_a) = c_p m(T_o - T_a) + C(T_o - T_a) \tag{28a}$$

When the heater is on

$$Q_{cool} + Q_{heat} = Q_{out} + Q_{lost} \tag{29}$$

or

$$c_p m(T_m - T_a) + Q_{heat} = c_p m(T_o - T_a) + C(T_o - T_a) \tag{29a}$$

The heat output Q_{heat} of the lamp used can be calculated

$$Q_{heat} = (15.5v)(1.12a)\left(\frac{w}{v\text{-}a}\right)\left(\frac{Btu}{1054w\text{-}sec}\right)\left(\frac{60sec}{min}\right)$$

$$Q_{heat} = 0.987 \approx 1 \text{ Btu/min.}$$

Inserting any given set of temperature data and the value of the heat capacity of air at constant pressure (c_p), the unknowns m and C may be calculated. It is necessary that the flow m be the same in both conditions, while the temepratures vary.

APPENDIX V

EXPERIMENTAL RESULTS

The following graphs are the actual experimental data points taken during the testing. As explained in Chapter IV, Tests A, B, and C were open-loop tests and the final test was a closed-100p test of the complete system.

Open-loop Test A was to determine the temperature responses of the mixer and the box for a given pressure input applied to the right side of the flow amplifier. Figure 22 plots the temperature versus time responses for no control pressure input. When this condition reached equilibrium, a control pressure of 0.5 psig was entered and its response plotted in Figure 23. Subsequent tests at 1.0 and 1.5 psig control pressure are shown in Figure 24. Later in the testing a portion of Test A was repeated and the sensor pressure differential was recoreded in additon to the temperature changes for control pressures of 1.0 and 1.5 psig. These plots are shown in Figures 25 and 26.

Open-loop Test B was the same as Test A except that both the sensor pressure differential and the temperature responses were recorded for each data point. Figure 27 shows the thermal and pressure responses for a control pressure of 0.5 psig. Figures 28, 29 and 30 show the same responses for control pressure inputs of 1.0, 1.g and 2.0, and 3.0 psig respectively.

Test C was an open-loop test of the thermal response of the box and of the pressure response of the temprature sensor and pressure amplifiers

as a function of time. This response was taken as the box was heated up and again as it cooled to room temperature. Figure 31 shows the various temperatures and the output pressure differential of the sensor plotted against time for the box heating up. Figure 32 shows the same plots as the box cooled again. Eliminating the time variable, Figure 33 shows the temperature-pressure or input-output response of the sensor and pressure amplifiers as the box was heated and then cooled.

The final test was the complete closed-loop control system. The data taken in this test were the same as in Test C - the three temperatures and the sensor output pressure differential. This data is shown in Figure 34 for the box being heated, and Figure 35 for the bo x while cooling. From this data it is difficult to determine whether the control signal, T_{mix}, changes. If it does, it does not go in the proper direction. The lack of response of T_{mix} in Figure 34 indicates that either the gain somewhere in the system is very low, or that an amplifier has reached saturation and cannot provide any further compensation. In Figure 35 T_{mix} decreases after a while, instead of further increasing. This might be caused by the effect of increased control air flow mixing with the hot and cold air. The effect of increased control air flow attempting to cause further deflection of the power jet may actually be neutralizing the temperature of T_{mix}.

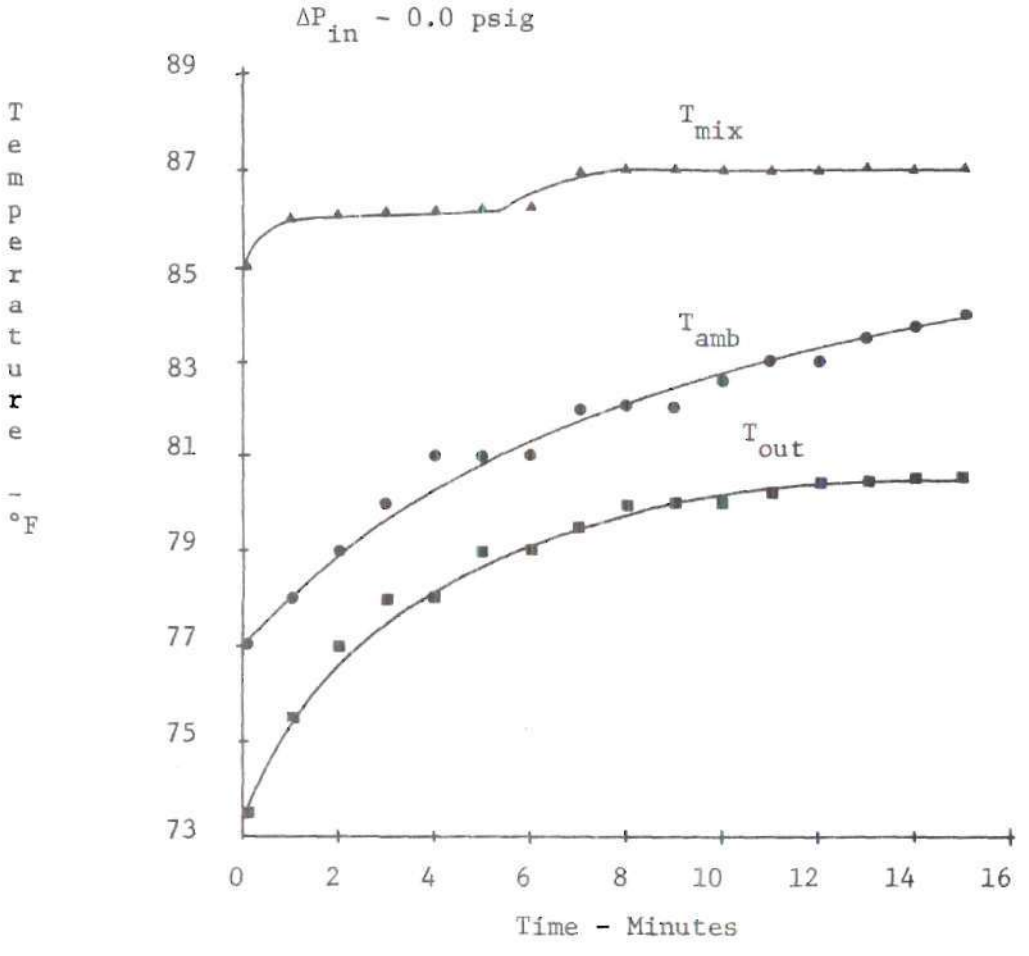

Figure 22. Test A, Open-Loop Temperature Response for no Input Pressure. Box Approaching Equilibrium from Room Temperature

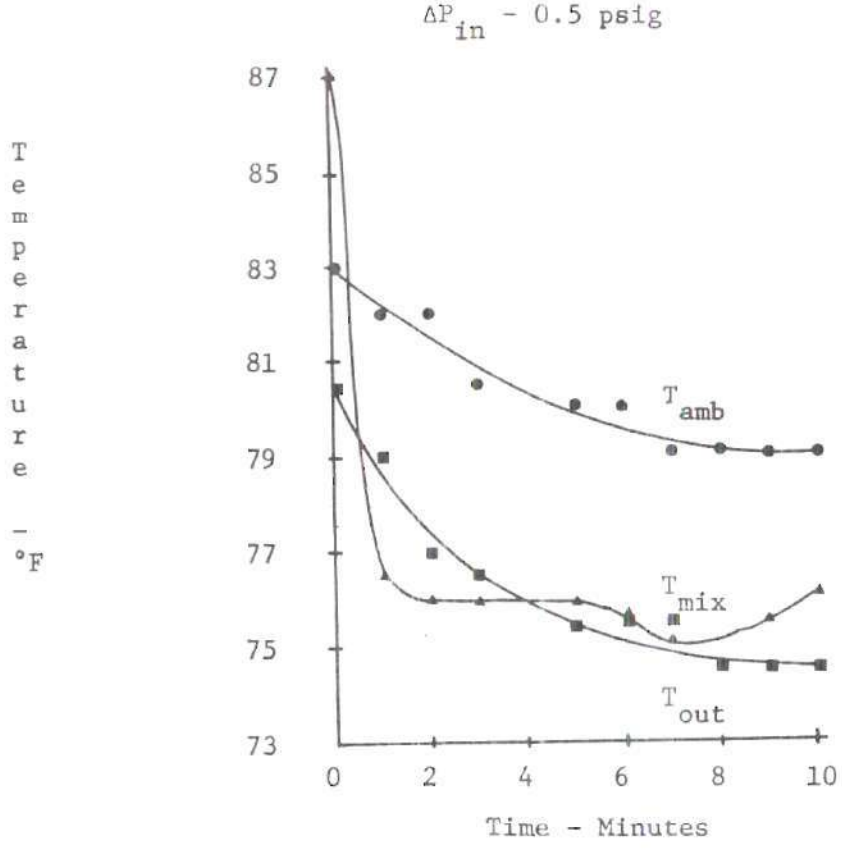

Figure 23. Test A, Open-Loop Temperature Response for Input Pressure of 0.5 psig

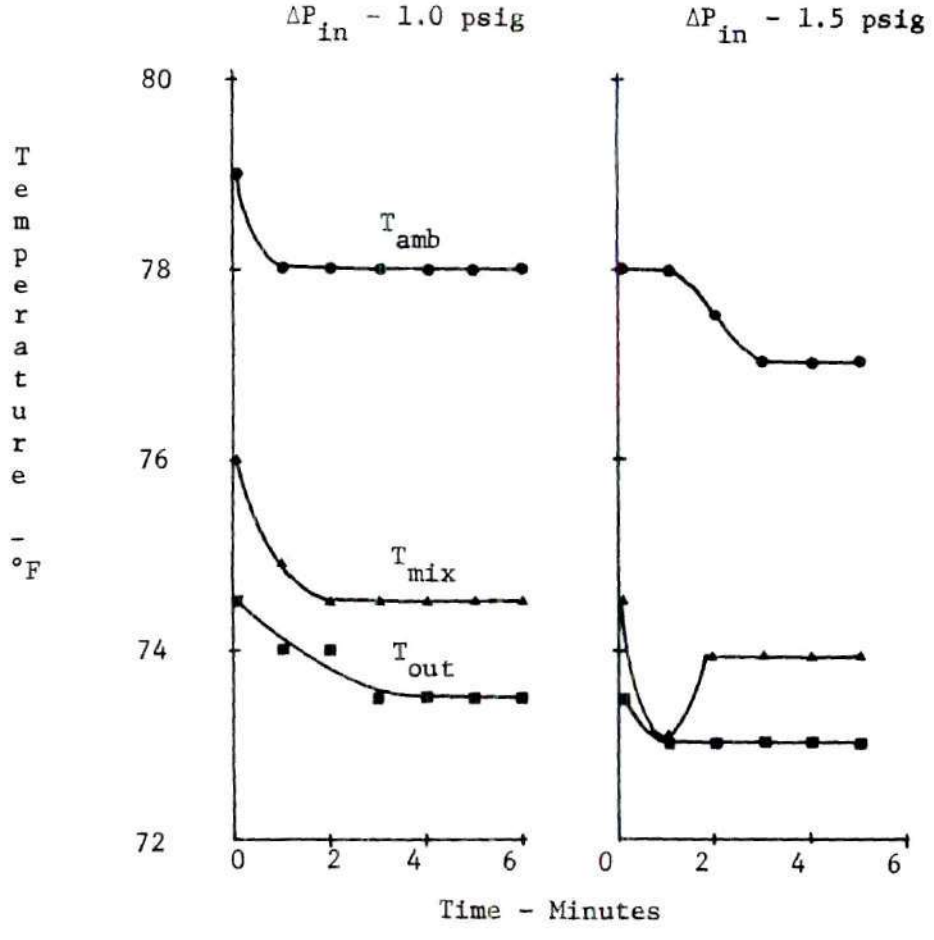

Figure 24. Test A, Open-Loop Temperature Response for Input Pressures of 1.0 and 1.5 psig

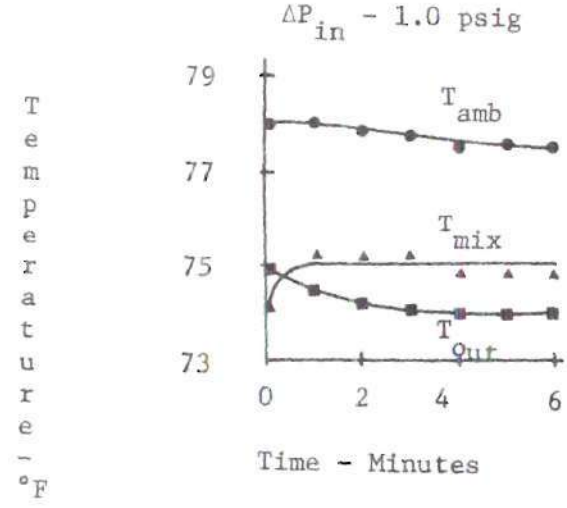

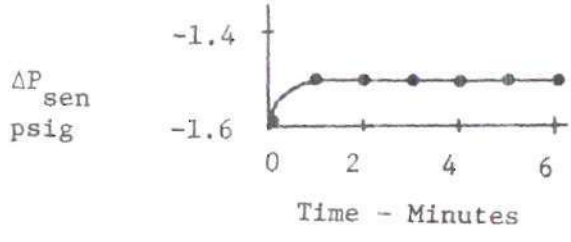

Figure 25. Test A, Open-Loop Temperature and Sensor Response for an Input of 1.0 psig

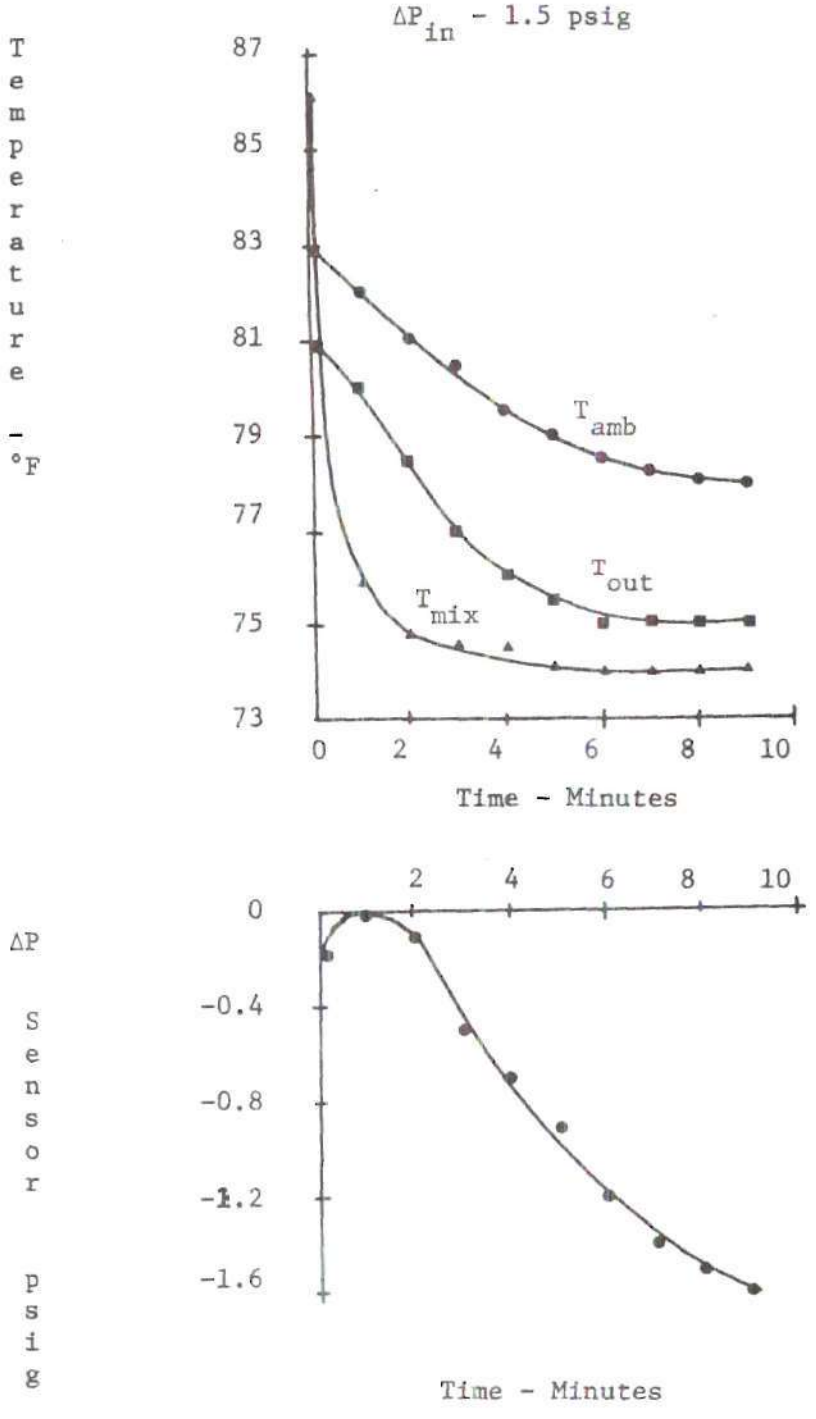

Figure 26. Test A, Open-Loop Temperature and Sensor Response for an input of 1.5 psig

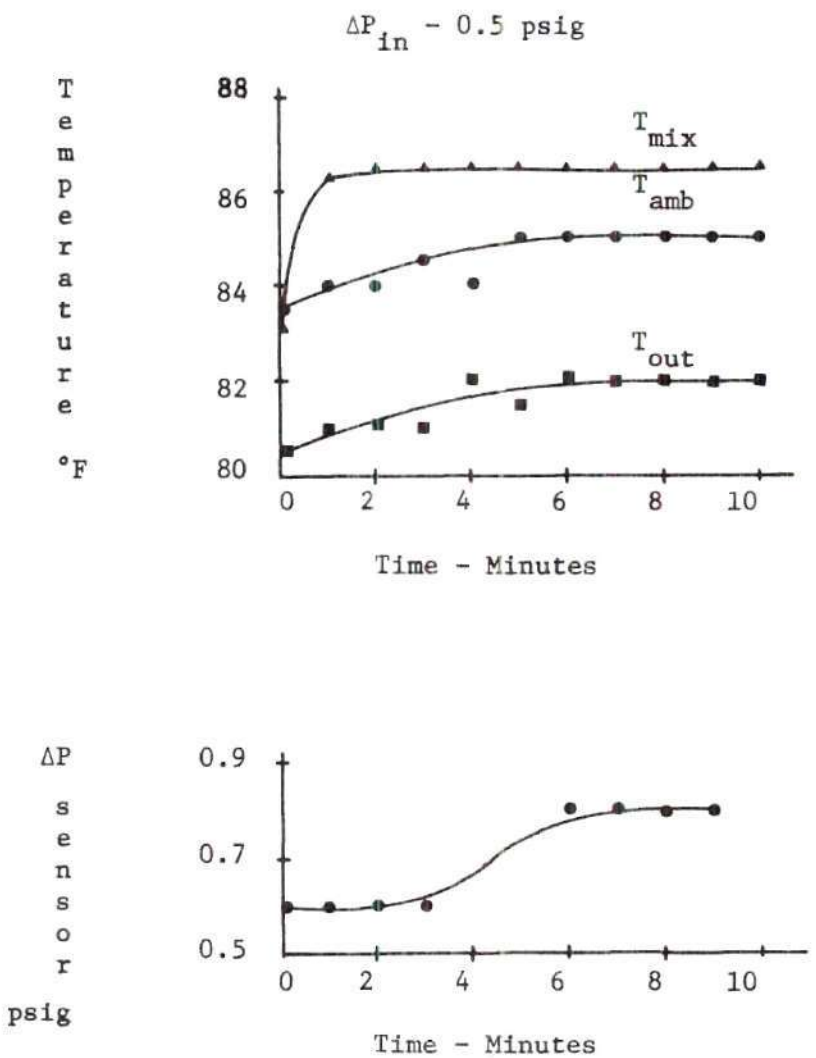

Figure 27. Test B, Open-Loop Temperature and Sensor Response for an Input Pressure of 0.5 psig

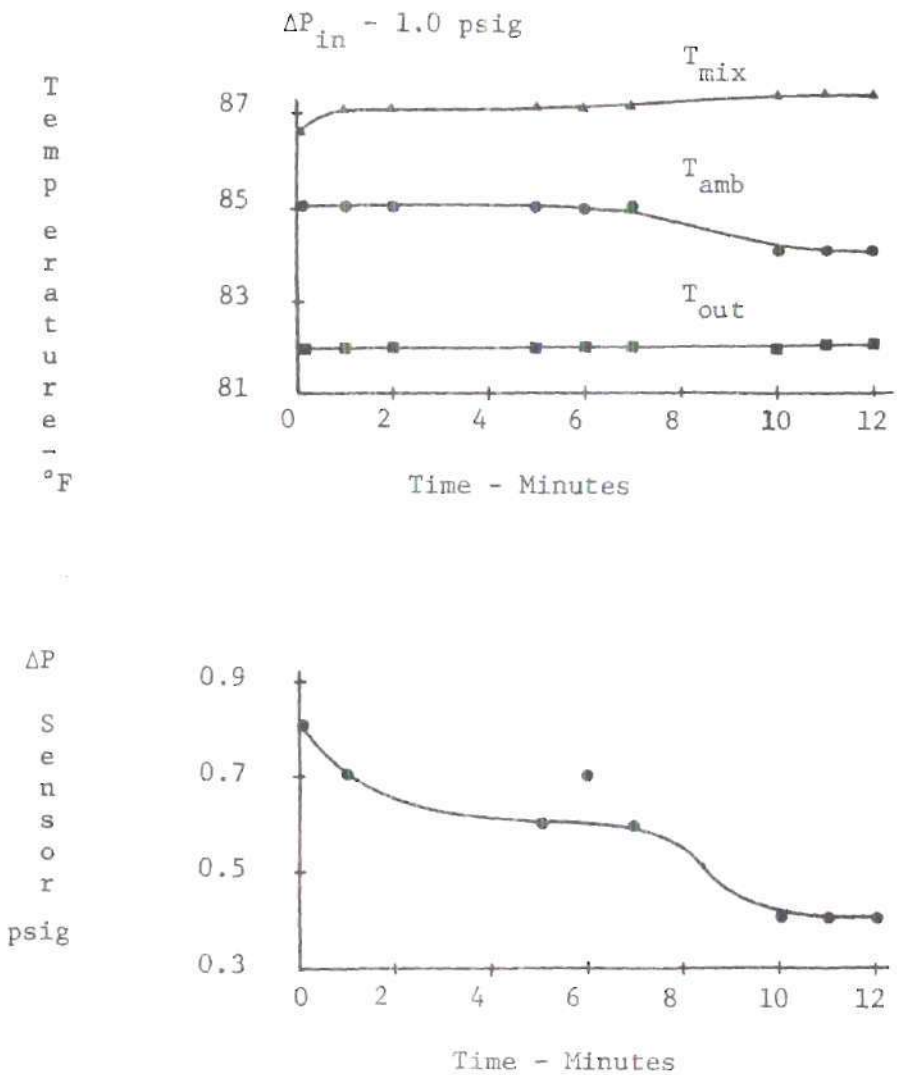

Figure 28. Test B, Open-Loop Temperature and Sensor Response for an Input Pressure of 1.0 psig

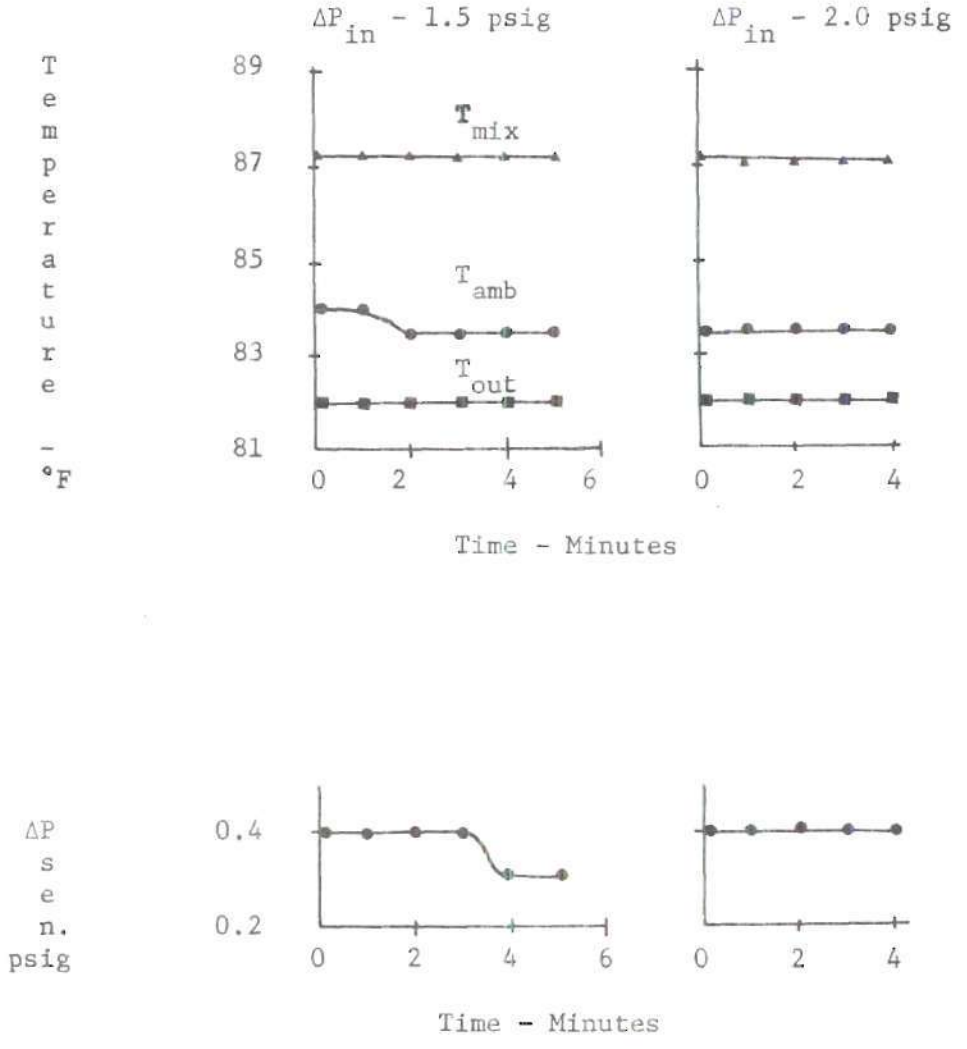

Figure 29. Test B, Open-Loop Temperature aned Sensor Response for Input Pressures of 1.5 and 2.0 psig

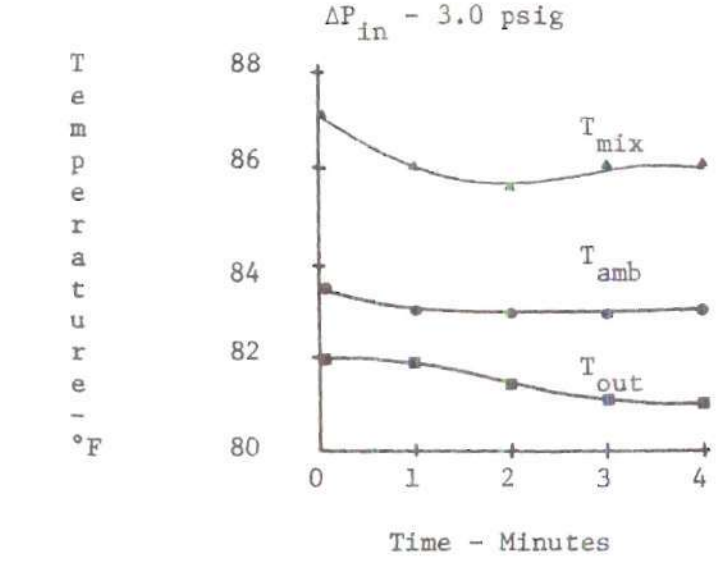

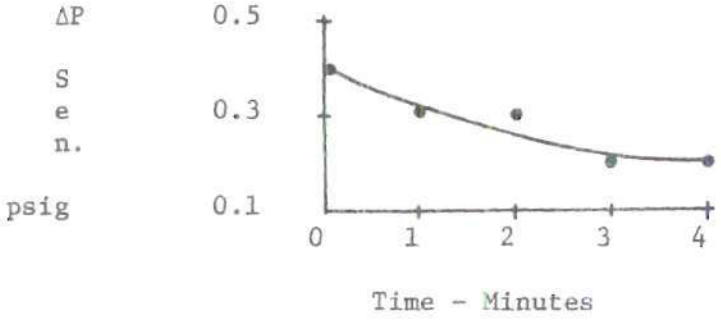

Figure 30. Test B, Open-Loop Temperature and Sensor Response for an Input Pressure of 3.0 psig

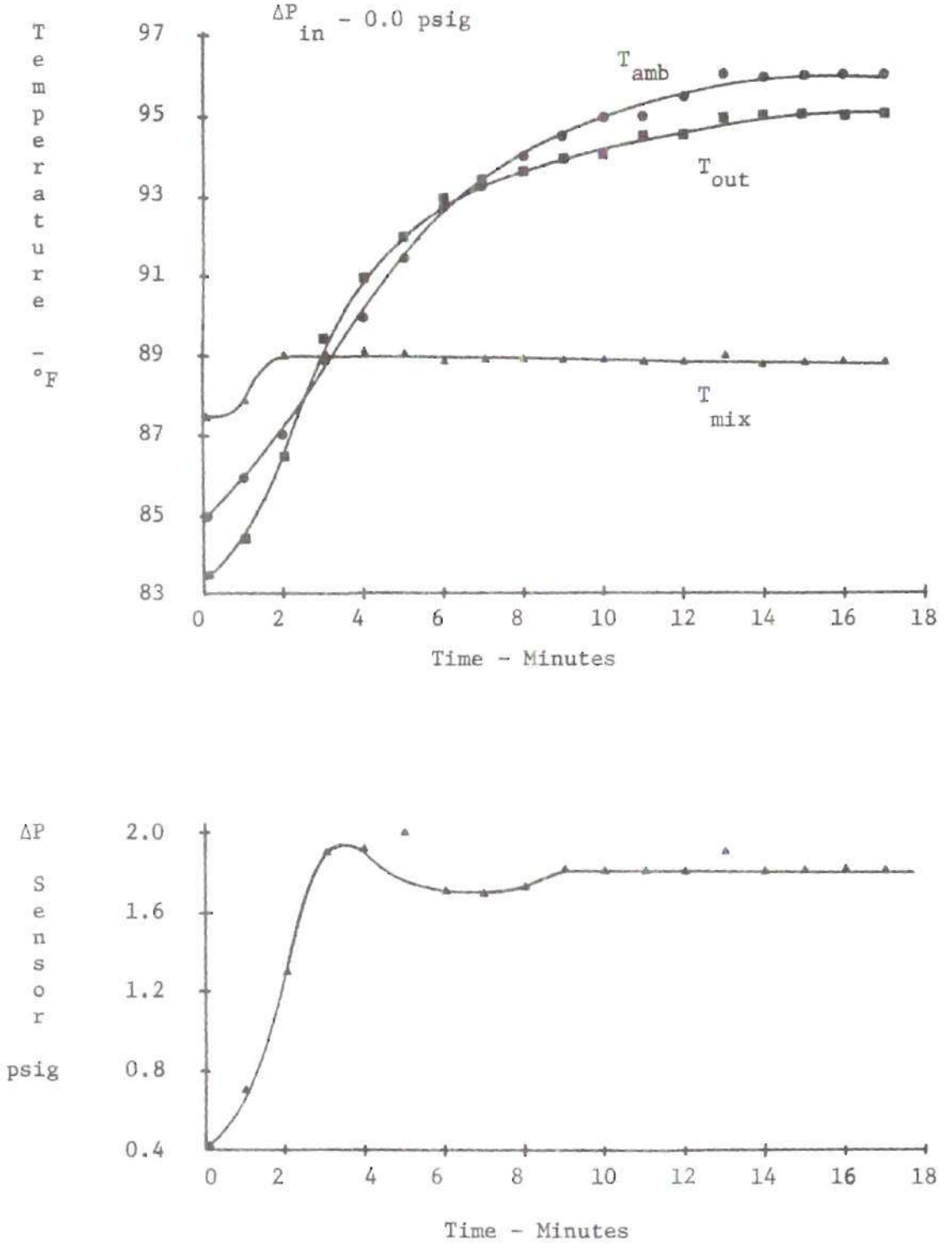

Figure 31. Test C, Open-Loop Temperature and Pressure Response of Box Heating from Room Temperature With Heater On. No Control Pressure Into the Flow Amplifier

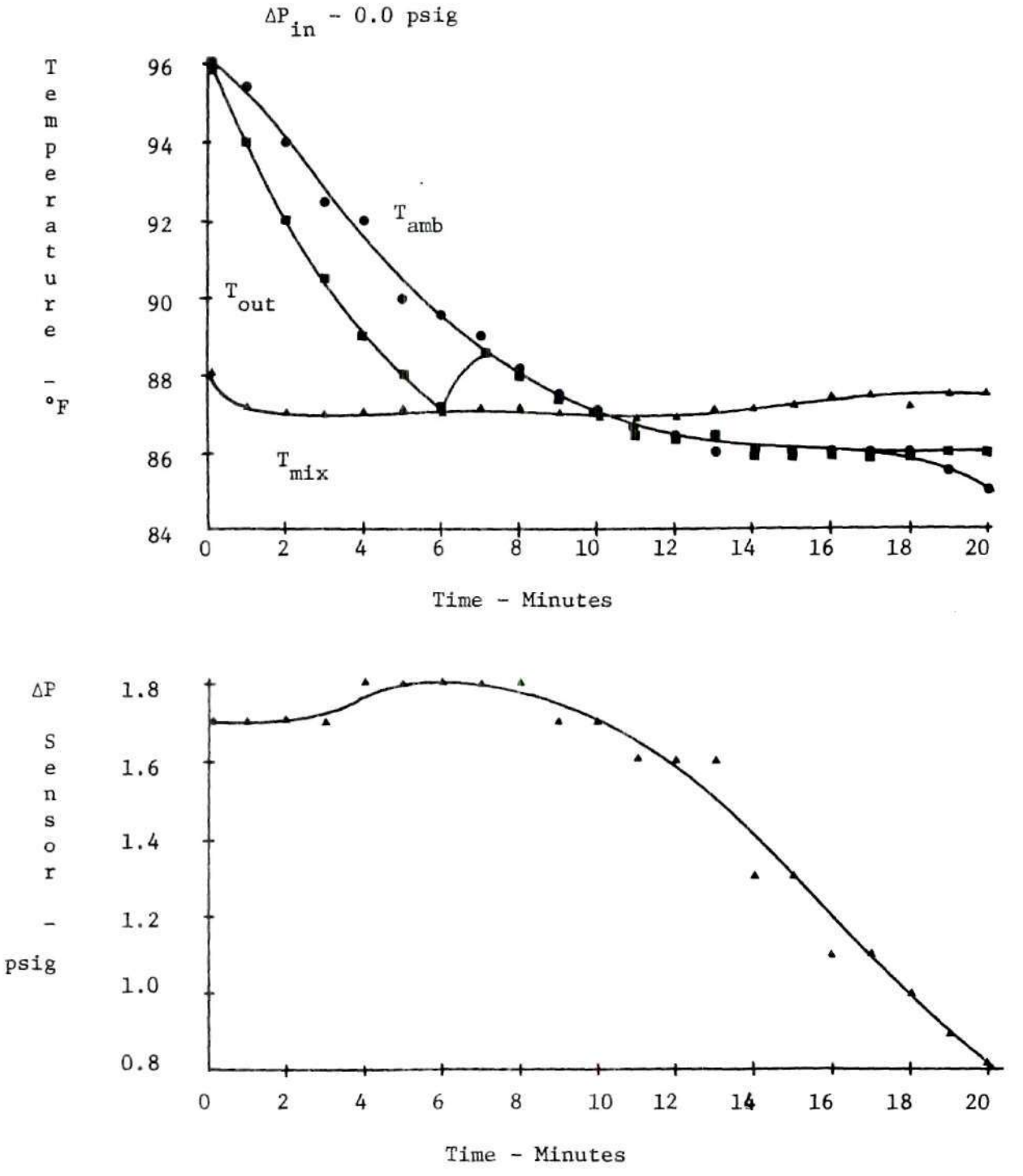

Figure 32. Test C, Open-Loop Temperature and Pressure Response of Box Cooling from a Warm Steady-State Condition. No Control Pressure into the Flow Amplifier

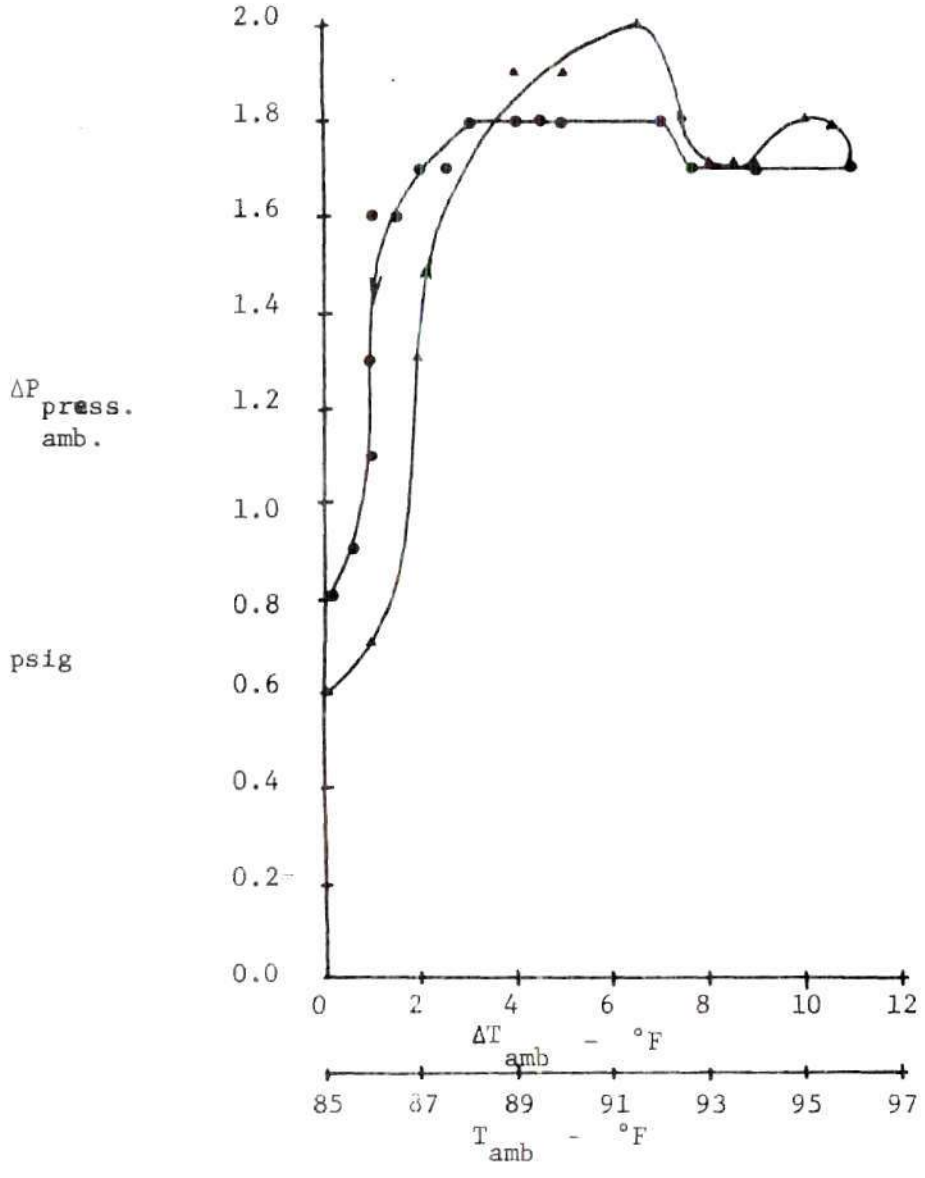

Figure 33. Test C, Open-Loop Response of Sensor and Pressure Amplifiers

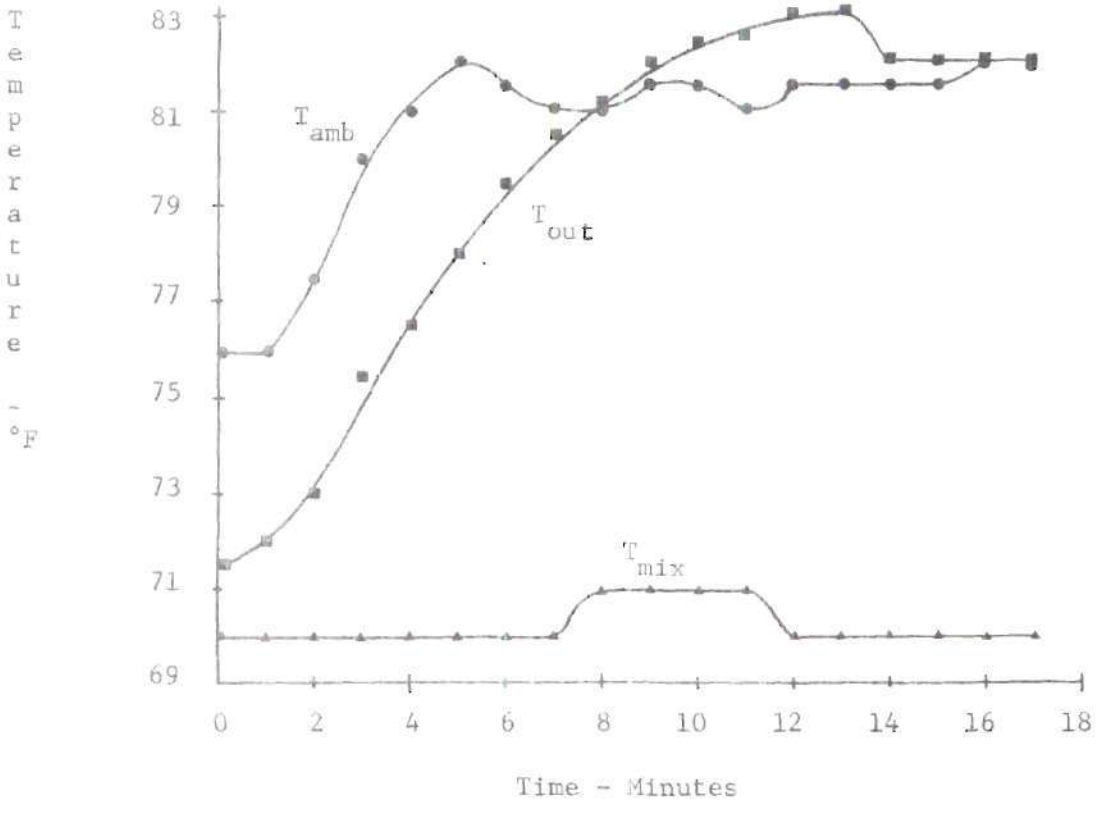

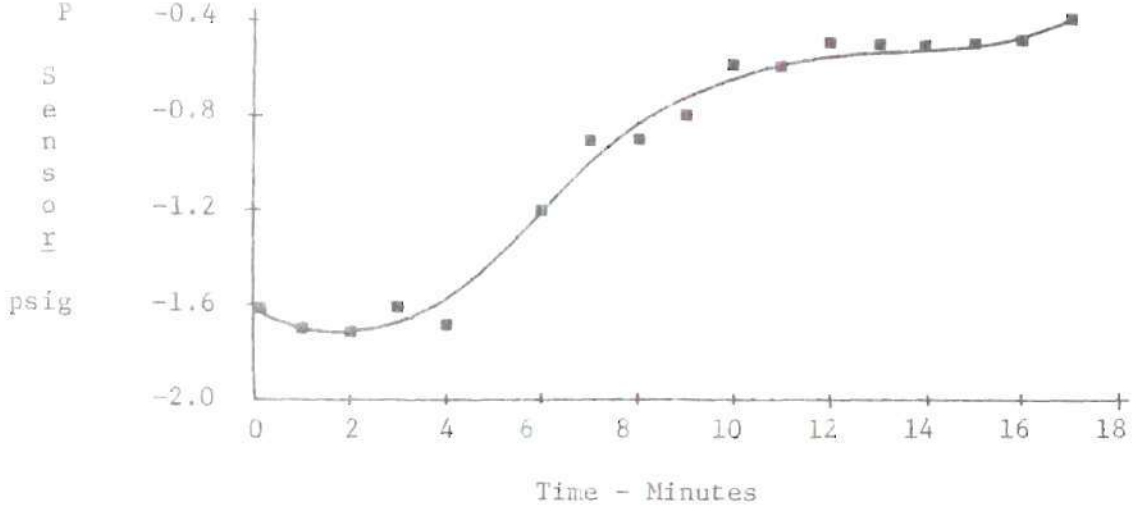

Figure 34. Closed-Loop Temperature and Pressure Response of Box While Heating

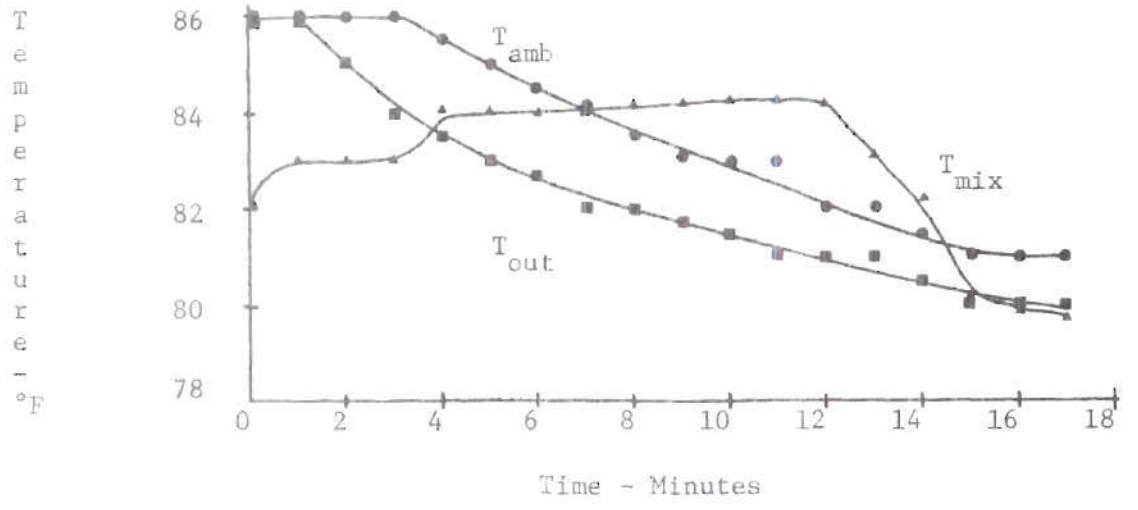

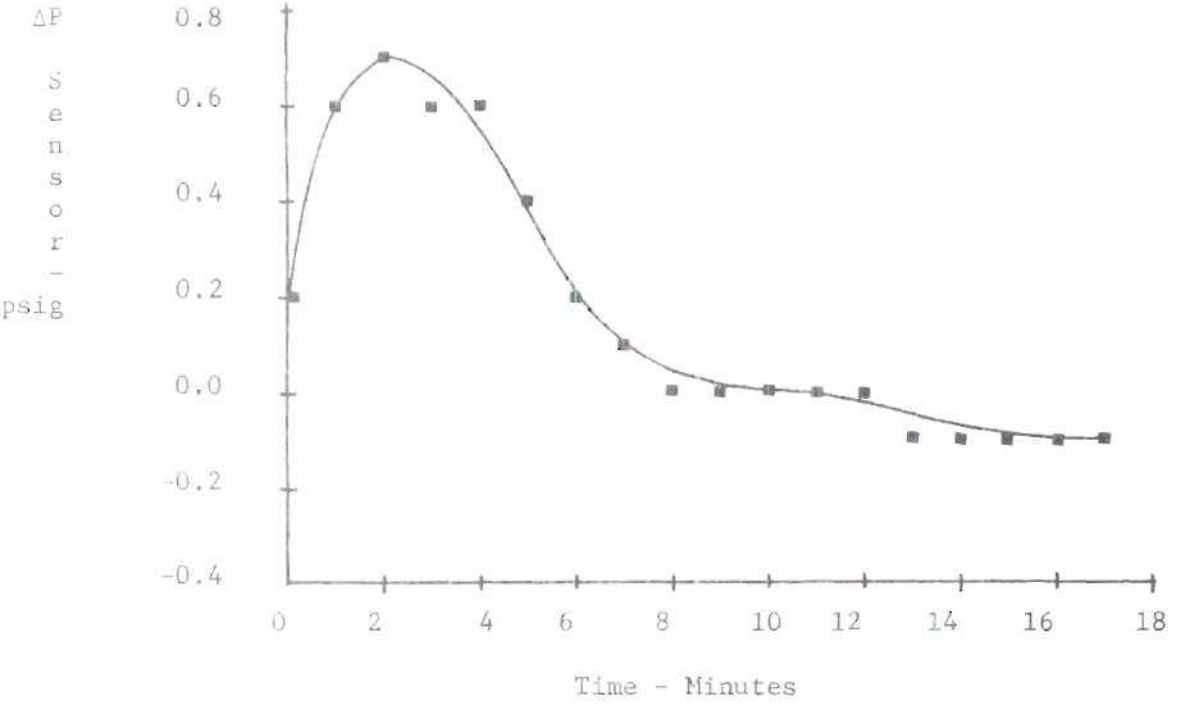

Figure 35. Closed-Loop Temperature and Pressure Response of Box While Cooling

APPENDIX VI

PHOTOGRAPHS OF EQUIPMENT

The following photographs show the experimental equipment as it was set up during the testing. Much of the equipment is set up on a temporoary basis for testing and is not meant to be for pemanent installation.

Figure 36 shows the entire equipment setup. The perforated metal mounting board is from a Corning FLUIDIKIT and is used to mount the amplifier stages and gauges for pressure monitoring. (See the close-up in Figure 37.) The wooden board on the tabel is the mounting for the main components of the system -- the Hilsch tube and controllers (see Figure 38). The temperature sensor and mixing tube shown on the table are inserted in the container where the temperature is to be monitored. These are also shown in the clos-up, Figure 38.

Figure 37 is a close-up of the amplifiers and pressure gauges. From top to bottom are shown the first and second stage pressure amplifiers (Corning proportional amplifiers), the flow amplifier, and the five pressure gauges from the FLUIDIKIT. The power relay on the left of the board is part of the FLUIDIKIT and is not a part of the circuit. The device in the top center of the board is a manifold for distribution of the control pressure.

Figure 38 is a close-up of the main system components. The white tube across the top of the board is the Hilsch Tube. The clamp on the vortex section is a temporary measure to eliminate pressure leaks developed in the latter stages of testing. The clamp on the rubber tubing section is for adjustment of the back pressure. The two hot and cold air controllers are

shown mounted on the board, the hot on the left and cold on the right. The hot and cold output tubes from the controllers are shown joining in the mixing tube. The mixing tube was developed for testing purposes so that the mixing temperature of the air entering the box could be measured by the thermocouple shown inside the tube. In the lower right hand corner is the temperature sensor. Its spiral bimetal and two nozzles can be easily seen. The two clamps shown sticking from behind the board on either side are the exhaust valves which make it possible to balance the hot and cold air supplied to the controllers, as noted to Chapter III.

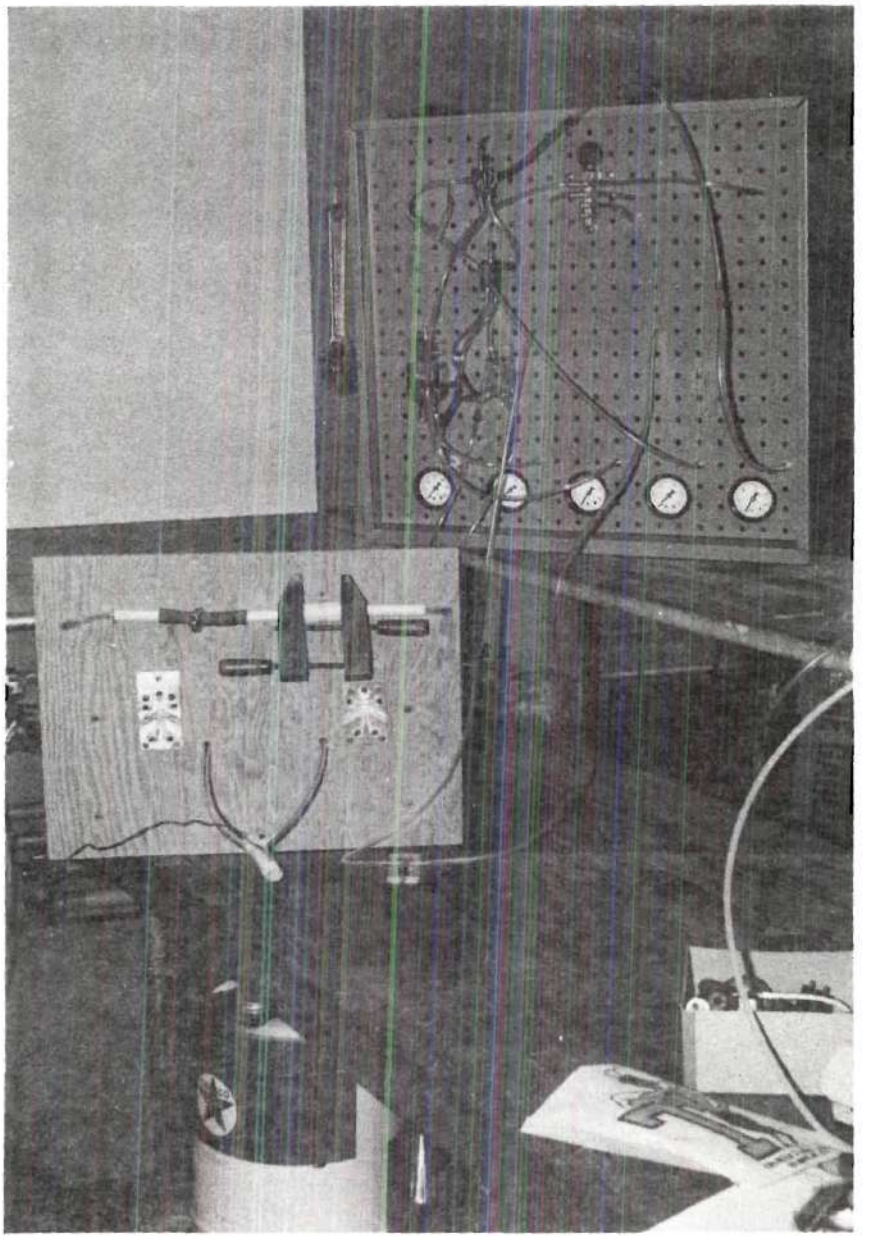

Figure 36 - Laboratory set-up of temperature control system. Box not shown.

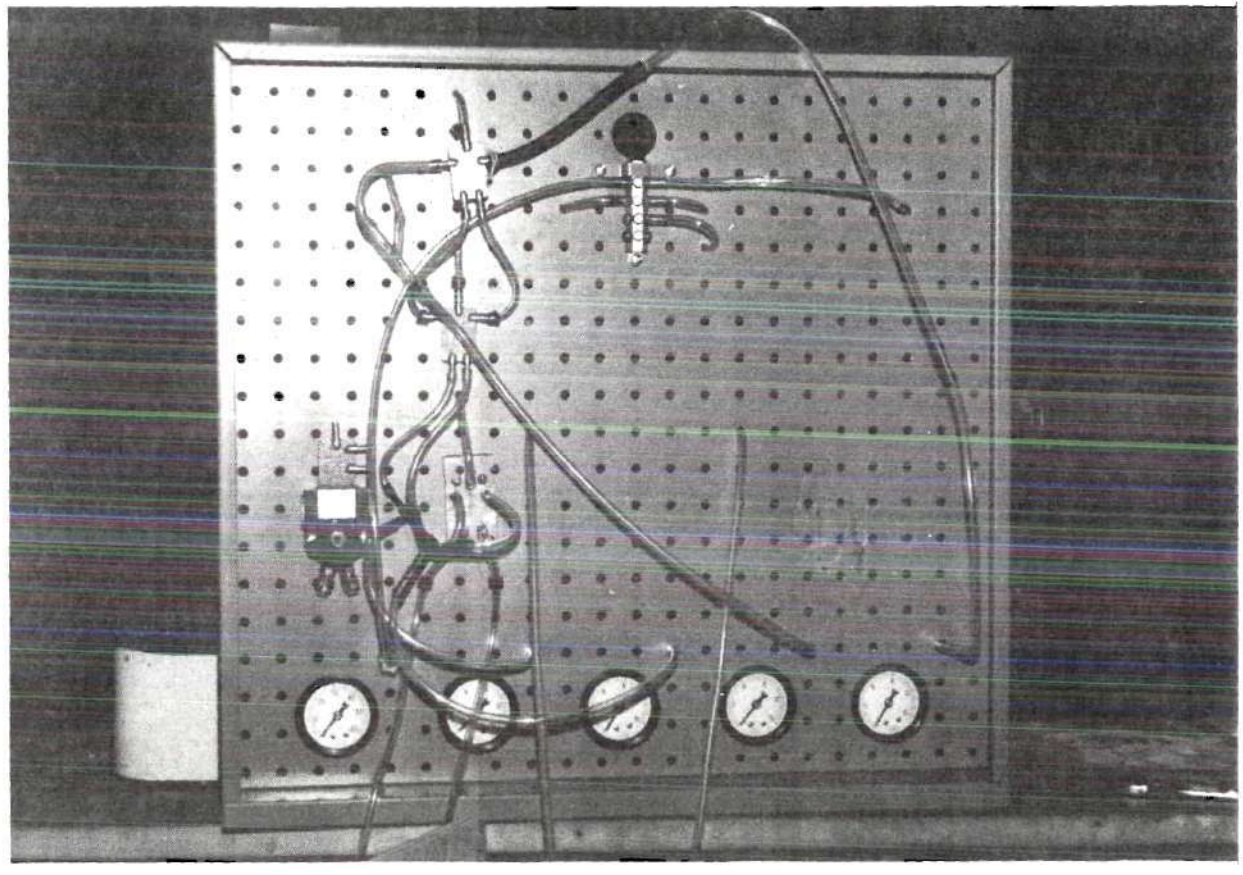

Figure 37 - Close-up of pressure amplifiers, flow amplifier, and pressure gauges.

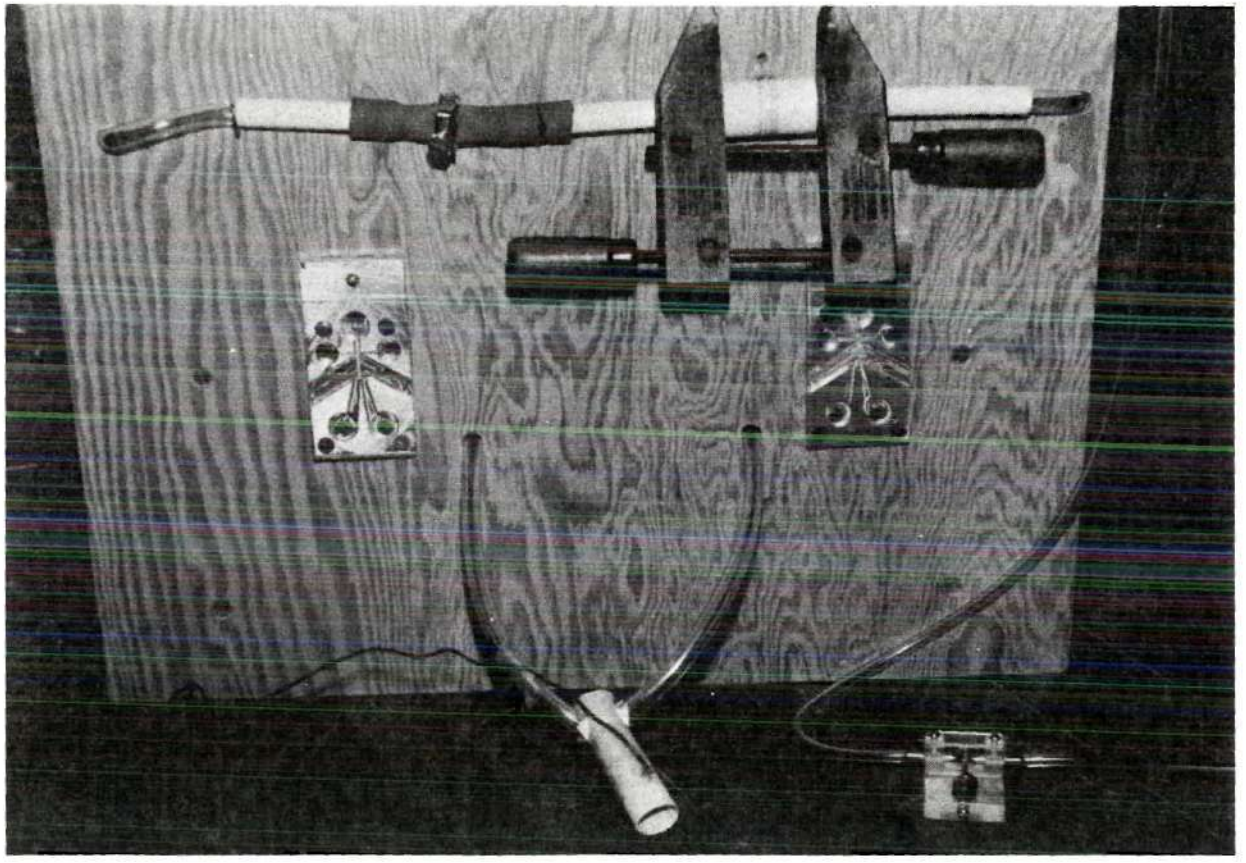

Figure 38 - Close-up of Hilsch tube, hot and cold controllers, mixing tube, and sensor.

BIBLIOGRAPHY

Literature Cited

1. M. G. Ranque, "Experiences sur la Detente Giratoire Avec Productions Simultanees d'un Echappement d'Air Chaud et d'Air Froid", Journal de Physique et le Radium, series 7, vol. 4, pt. 1, 1933, pp. 112s-115s.

2. R. Hilsch, "The Use of the Expansion of Gases in a Centrifugal Field as Cooling Process", Review of Scientific Instruments, vol. 18, No. 2, Feb. 1947, pp. 108-113.

3. Edward R. Searles, ed., "Vortex Tube Cooling for Supersonic Craft", American Society of Heating, Refrigerating and Air-conditioning Engineers Journal, vol. 3, no. 2, Feb. 1961, p. 99.

4. T. B. Metcalfe, "The Vortex Tube -- Heat Source and Sink", British Chemical Engineering, vol. 11, no. 8, Aug. 1966, pp. 854-855.

5. R. E. Bowles, "State of the Art of Pure Fluid Systems", Fluid Jet Control Devices, Symposium on Fluid Jet Control Devices, Winter Annual Meeting of American Society of Mechanical Engineers, New York, New York, November 28, 1962, pp. 7-22.

6. E. M. Dexter, "An Analog Pure Fluid Amplifier", ibid, pp. 41-49.

7. R. J. Reilly and F. A. Moynihan, "Notes on a Proportional Fluid Amplifier:, ibid, pp. 51-57.

8. D. McCloy and S. L. Dickerson, Investigation of the Application of Fluidics for Flight Control Subsystems, Report No. ER-9761, Lockheed-Georgia Company, February 1, 1968.

9. Carl R. Halbach, Ben A. Otsap, and Richard A. Thomas, "A Pressure Insensitive Fluidic Temperature Sensor", Advances in Fluidics, The 1967 Fluidics Symposium, Fluidics Committee, Fluids Engineering and Controls Divisions, ASME, Chicago, Ill., May 9-11, 1967, pp. 298-312.

10. John F. Blackburn, Gerhard Rethoff, and J. Lowen Shearer, Fluid Power Control, The Technology Press of M.I.T. and John Wiley & Sons, Inc., New York, 1960, pp. 214-277.

11. Blaine W. Andersen, The Analysis and Design of Pneumatic Systems, John Wiley & Sons, Inc., New York, 1967, pp. 1-102.

12. John E. Gibson and Franz B. Tuteur, Control System Components, John Wiley & Sons, Inc., New York, 1967, pp. 1-102.

13. M. P. Blaber, "A Simply Constructed Vortex Tube for Producing Hot and Cold Air Streams", Journal of Scientific Instruments, vol. 27, 1950, pp. 168-169.

14. Chace Thermostatic Bimetal Design Catalog, W. M. Chace Co., 1967, pp. 23-34, 58.

15. Perry Githens, ed., "Maxwell's Demon Comes to Life", Popular Science, vol. 150, no. 5, May 1947, pp. 144-146.

16. D. S. Webster, "An Analysis of the Hilsch Vortex Tube", Refrigerating Engineering , vol. 58, 1950, pp. 163-170.

17. C. D. Fulton, "Ranque's Tube", Journal of American Society of Refrigerating Engineers, Refrigerating Engr., vol. 58, 1950, pp. 473-479.

18. C. D. Fulton, "Comments on the Vortex Tube", Refrigerating Engr., vol. 59, 1951, p. 984.

19. George W. Scheper, Jr., "The Vortex Tube -- Internal Flow Data and a Heat Transfer Theory", Journal of ASRE, Refrigerating Engr., vol. 59, October 1951, pp. 985-989, 1018.

20. J. J. Van Deemter, "On the Theory of the Ranque-Hilsch Cooling Effect" Applied Scientific Research, section A, vol. 3, 1952, pp. 174-196.

21. C. D. Pengelley, Flow in a Viscous Vortex, Report 494C-1, TN 56-126, Southwest Research Institute, 1956.

22. J. E. Lay, "An Experimental and Analytical Study of Vortex-Flow Temperature Separation by Superposition of Spiral and Axial Flows, Part I", Transactions of the ASME, August 1959, pp. 202-221.

23. R. G. Deissler and M. Perlmutter, "Analysis of the Flow and Energy Separation in a Turbulent Vortex", International Journal of Heat & Mass Transfer, vol. 1, no. 2-3, Aug. 1960, pp. 173-191.

24. A. I. Gulyaev, "Vortex Tubes and the Vortex Effect (Ranque Effect)", Soviet Physics - Technical Physics, vol. 10, no. 10, April 1966, pp. 1441-1449.